

**Fabrication and Permeation Analysis of Polysulfone (PSf)  
Modified Cellulose Triacetate (CTA) Blend Membranes for  
CO<sub>2</sub> Separation from Methane**



By

Humais Roafi

(Registration No: 00000362913)

Department of Chemical Engineering

School of Chemical and Materials Engineering

National University of Sciences & Technology (NUST)

Islamabad, Pakistan

(2024)

**Fabrication and Permeation Analysis of Polysulfone (PSf)  
Modified Cellulose Triacetate (CTA) Blend Membranes for  
CO<sub>2</sub> Separation from Methane**



By

Name: Humais Roafi

Registration No: 00000362913

A thesis is submitted to the National University of Sciences and Technology,  
Islamabad, in partial fulfilment of the requirements of the degree of

Master of Science in

Chemical Engineering

Supervisor Name: Dr. Ayesha Raza

Co-Supervisor: Dr. Sarah Farrukh

School of Chemical and Materials Engineering

National University of Sciences and Technology (NUST)

Islamabad, Pakistan

(2024)



THESIS ACCEPTANCE CERTIFICATE

Certified that final copy of MS thesis written by Mr Humals Roafl (Registration No 00000362913), of School of Chemical & Materials Engineering (SCME) has been vetted by undersigned, found complete in all respects as per NUST Statues/Regulations, is free of plagiarism, errors, and mistakes and is accepted as partial fulfillment for award of MS degree. It is further certified that necessary amendments as pointed out by GEC members of the scholar have also been incorporated in the said thesis.

Signature: 

Name of Supervisor: Dr Ayesha Raza

Date: 28-02-2024

Signature (HOD): 

Date: 28/2/24

Signature (Dean/Principal): 

Date: 28.2.2024



Form TH-1

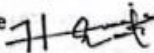
**National University of Sciences & Technology (NUST)****MASTER'S THESIS WORK**

Formulation of Guidance and Examination Committee (GEC)

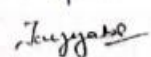


Name: Humais Roafi NUST Reg No: 00000362913  
Department: Department of Chemical Engineering Specialization: Master of Science in Chemical Engineering  
Credit Hour Completed: 18.0 CGPA: 3.58

**Course Work Completed**

S/No:Code:	Title:	Core/Elective:	CH:	Grade:
1. CHE-847	Chemical Kinetics & Reactor Design	Compulsory	3.0	B
2. CHE-843	Separation Processes In Che	Compulsory	3.0	B
3. RM-898	Research Methodology	Additional	2.0	Q
4. ENE-809	Waste Water Treatment & Design	Elective	3.0	B+
5. EME-921	Momentum, Heat & Mass Transfer In Chemical Engineering Separation Processes	Compulsory	3.0	A
6. CHE-853	Green Process Engineering	Elective	3.0	A
7. CHE-873	Membrane Technology	Elective	3.0	A

Date 23 - Nov - 2022Student's Signature **Thesis Committee**

- Name: Sarah Farrukh (Supervisor)  
Department: Department of Chemical Engineering
- Name: Ayesha Raza (Cosupervisor)  
Department: Department of Chemical Engineering
- Name: Tayyaba Noor (Internal)  
Department: Department of Chemical Engineering
- Name: Sofia Javed (Internal)  
Department: Department of Materials Engineering

Signature Signature Signature Signature Date: 23 - Nov - 2022Signature of Head of Department: **APPROVAL**Date: 23 - Nov - 2022Signature of Dean/Principal: 



MASTER'S THESIS WORK

We hereby recommend that the dissertation prepared under our supervision by

Regn No & Name: 00000362913 Humais Roafi

Title: Fabrication and Permeation Analysis of Polysulfone (PSf) Modified Cellulose Triacetate (CTA) Blend Membranes for CO<sub>2</sub> Separation from Methan.

Presented on: 25 Jan 2024 at: 1430 hrs in SCME Seminar Hall

Be accepted in partial fulfillment of the requirements for the award of Master of Science degree in Chemical Engineering.

Guidance & Examination Committee Members

Name: Dr Sofia Javed

Signature: [Signature]

Name: Dr Tayyaba Noor

Signature: [Signature]

Name: Dr Sarah Farrukh (Co-Supervisor)

Signature: \_\_\_\_\_

Supervisor's Name: Dr Ayesha Raza

Signature: [Signature]

Dated: \_\_\_\_\_ 25-1-2024

[Signature]  
Head of Department  
Date 14/2/24

[Signature]  
Dean/Principal  
Date 16.2.24

## **AUTHOR'S DECLARATION**

I Humais Roafi hereby state that my MS thesis titled “Fabrication and Permeation Analysis of Polysulfone (PSf) Modified Cellulose Triacetate (CTA) Blend Membranes for CO<sub>2</sub> Separation from Methane” is my own work and has not been submitted previously by me for taking any degree from the National University of Sciences and Technology, Islamabad, or anywhere else in the country/world.

At any time, if my statement is found to be incorrect even after I graduate, the university has the right to withdraw my MS degree.

Name: Humais Roafi

Date: 25-01-2024

## **PLAGIARISM UNDERTAKING**

I solemnly declare that the research work presented in the thesis titled “Fabrication and Permeation Analysis of Polysulfone (PSf) Modified Cellulose Triacetate (CTA) Blend Membranes for CO<sub>2</sub> Separation from Methane” is solely my research work with no significant contribution from any other person. Small contribution/ help wherever taken has been duly acknowledged and that complete thesis has been written by me.

I understand the zero-tolerance policy of the HEC and the National University of Sciences and Technology (NUST), Islamabad towards plagiarism. Therefore, I as an author of the above-titled thesis declare that no portion of my thesis has been plagiarized and any material used as reference is properly referred to/cited.

I undertake that if I am found guilty of any formal plagiarism in the above-titled thesis even after the award of my MS degree, the University reserves the right to withdraw/revoke my MS degree and that HEC and NUST, Islamabad has the right to publish my name on the HEC/University website on which names of students are placed who submitted plagiarized thesis.

Name: Humais Roafi

Date: 25-01-2024

## DEDICATION

By the grace of **Almighty Allah**, who is the most Compassionate and Merciful.

With heartfelt dedication, I offer this achievement to my Parents, whose unwavering love and support have fortified my journey. To my cherished spouse, your unwavering encouragement has been my steadfast motivation.

To my exceptional supervisor, Dr. Sarah Farrukh, your invaluable guidance has illuminated my path. To my esteemed lab mates, your camaraderie and shared endeavors have enriched this journey.

I also extend my profound gratitude to my dear friend Kinza Hamid, whose substantial contributions have been instrumental. This accomplishment stands as a testament to the collective contributions of everyone, inspiring me to continually strive for excellence.



## ACKNOWLEDGEMENTS

Blessings foremost, I extend my utmost gratitude to **Allah Almighty**, whose unwavering blessings and guidance have illuminated my path and fueled my determination. Your divine guidance has been my source of strength and inspiration, and for that, I am eternally grateful.

I would like to express my sincere appreciation to my supervisor, Dr. Sarah Farrukh, for her exceptional mentorship, unwavering encouragement, and profound insights. Your expertise and dedication have been pivotal in shaping my research and fostering my growth as a scholar. I am truly fortunate to have had the privilege to learn from you. I am equally indebted to my co-supervisor, my sincere gratitude to Dr. Ayesha Raza for her invaluable guidance, which has been instrumental in refining and broadening my perspectives. I also extend heartfelt appreciation to the esteemed members of the GEC, Dr. Tayyaba and Dr. Sofia Javed, whose constructive feedback and dedication to academic excellence have greatly enhanced the quality of my research.

My gratitude extends to my Parents, whose unwavering love, encouragement, and sacrifices have been the cornerstone of my journey. Your belief in me has been my driving force, and I am humbled by your constant support.

To my dear best friend Kinza Hamid, your invaluable assistance, insightful discussions, and dedicated efforts have been nothing short of remarkable. Your willingness to lend a helping hand has been a source of inspiration. Your contributions have played a significant role in shaping this achievement, and I am deeply thankful for your friendship and for everything you have done.

I would also like to acknowledge the support and assistance of the lab support staff at SCME, whose dedication has ensured a conducive research environment. My heartfelt thanks to my fellow lab mates and colleagues who have shared in this journey. Your camaraderie, exchange of ideas, and collaborative spirit have enriched my experience and made this journey memorable.

## TABLE OF CONTENTS

<b>ACKNOWLEDGEMENTS</b> .....	<b>IX</b>
<b>TABLE OF CONTENTS</b> .....	<b>X</b>
<b>LIST OF FIGURES</b> .....	<b>XII</b>
<b>LIST OF TABLES</b> .....	<b>XIII</b>
<b>LIST OF ACRONYMS AND SYMBOLS</b> .....	<b>XIV</b>
<b>ABSTRACT</b> .....	<b>XV</b>
<b>1. CHAPTER 1 INTRODUCTION</b> .....	<b>1</b>
1.1 Background .....	1
1.2 Consumption of Natural Gas.....	3
1.3 Requirement of CO <sub>2</sub> Separation from Natural Gas.....	5
1.4 Techniques used for the Refinement of NG.....	5
1.4.1 Pressure Swing Absorption .....	6
1.4.2 Cryogenic Distillation .....	8
1.4.3 Membrane Technology.....	8
1.5 Motivation.....	11
1.6 Objective .....	11
<b>2. CHAPTER 2 LITERATURE REVIEW</b> .....	<b>13</b>
2.1 Membrane Materials .....	13
2.1.1 Polymeric Membranes .....	14
2.1.2 In-Organic Membranes .....	16
2.2 Mixed Matric Membranes.....	18
2.2.1 Fillers for Mixed Matrix Membranes (MMM) .....	19
2.3 Blend Membranes .....	23
2.4 Membrane Modules .....	25
<b>3. CHAPTER 3 MATERIALS AND METHODS</b> .....	<b>28</b>
3.1 Materials Utilized.....	28

3.2	Membrane Fabrication .....	28
3.2.1	Pristine and Blend Membranes Fabrication .....	28
3.3	Gas Permeation .....	30
<b>4.</b>	<b>CHAPTER 4 MEMBRANE CHARACTERIZATION .....</b>	<b>32</b>
4.1	Fourier Transform Infrared Spectroscopy .....	32
4.2	Scanning Electron Microscope .....	32
4.3	Ultimate Tensile Strength.....	34
4.4	X-ray diffraction (XRD) .....	35
<b>5.</b>	<b>CHAPTER 5 RESULT AND DISCUSSIONS .....</b>	<b>36</b>
5.1	FTIR Analysis .....	36
5.2	XRD Analysis .....	37
5.3	Ultimate Tensile Strength (UTS) Analysis.....	39
5.4	Scanning Electron Microscopy (SEM) Analysis.....	40
5.5	Gas Permeation Analysis.....	42
5.6	Performance Comparison.....	46
<b>6.</b>	<b>CHAPTER 6 CONCLUSION .....</b>	<b>48</b>
<b>7.</b>	<b>REFERENCES.....</b>	<b>50</b>

## LIST OF FIGURES

<b>Figure 1.1:</b> CO <sub>2</sub> Emissions from combustion of fuel and industrial activities, 1900-2022.....	1
<b>Figure 1.2:</b> Percentage contribution of different sources used for power generation.	2
<b>Figure 1.3:</b> Natural Gas Consumption around the world [1] .....	5
<b>Figure 1.4:</b> Process Flow Diagram of PSA Process .....	7
<b>Figure 1.5:</b> Process Flow Diagram of Cryogenic Distillation.....	8
<b>Figure 1.6:</b> Amine Sweetening PFD .....	9
<b>Figure 1.7:</b> Gas penetration across a membrane .....	9
<b>Figure 2.1:</b> Robeson plot for gas pair (CO <sub>2</sub> /CH <sub>4</sub> ) Separation [10].....	13
<b>Figure 2.2:</b> Schematic diagram of an ideal MMM.....	18
<b>Figure 2.3:</b> Gas Permeability of CO <sub>2</sub> from different wt% of TiO <sub>2</sub> .....	21
<b>Figure 3.1:</b> Cellulose-triacetate Structure[36].....	28
<b>Figure 3.2:</b> Polysulfone Structure[37].....	28
<b>Figure 3.3:</b> Fabrication of CTA/PSf Blend Membranes.....	29
<b>Figure 3.4:</b> Permeation Equipment Flow Diagram .....	31
<b>Figure 4.1:</b> Working of Fourier Transform Infra-Red spectroscopy. ....	32
<b>Figure 4.2:</b> Scanning Electron Microscope Analysis .....	33
<b>Figure 4.3:</b> Ultimate Tensile Strength Machine .....	34
<b>Figure 4.4:</b> X-ray diffraction (XRD).....	35
<b>Figure 5.1:</b> FTIR Results of Pristine CTA, PSf and CTA/PSf Blend Membranes ....	37
<b>Figure 5.2:</b> XRD Results of Pristine and CTA/PSf Blend Membranes.....	38
<b>Figure 5.3:</b> Ultimate Tensile Strength Results of Pristine CTA, PSf, and CTA/PSf Blend Membranes .....	39
<b>Figure 5.4:</b> SEM surface micrographs of (A)= 2wt% CTA/PSf, (B)= 4wt% CTA/PSf, (C)= 6wt% CTA/PSf, (D)= 8wt% CTA/PSf, (E)= 10wt% CTA/PSf.....	41
<b>Figure 5.5:</b> SEM Cross-Sectional micrographs of (A)= 2wt% CTA/PSf, (B)= 4wt% CTA/PSf, (C)= 6wt% CTA/PSf, (D)= 8wt% CTA/PSf, (E)= 10wt% CTA/PSf.....	42
<b>Figure 5.6:</b> Permeabilities of CO <sub>2</sub> .....	44
<b>Figure 5.7:</b> Permeabilities of CH <sub>4</sub> .....	45
<b>Figure 5.8:</b> Selectivity of CO <sub>2</sub> /CH <sub>4</sub> .....	46
<b>Figure 5.9:</b> Performance comparison graph for all the samples prepared. ....	47

## LIST OF TABLES

<b>Table 1.1:</b> Correlation between population (in thousands) and energy consumption (in thousands of metric tons of oil equivalent)[3] .....	3
<b>Table 1.2:</b> Typical Natural gas Composition[4] .....	4
<b>Table 1.3:</b> Materials used for pressure swing Adsorption .....	7
<b>Table 2.1:</b> Commercially used membrane material for impurity removal from natural gas. ....	15
<b>Table 2.2:</b> Characteristics, cons, and types of polymer membranes.....	16
<b>Table 2.3:</b> Pros and Cons of inorganic membranes .....	17
<b>Table 2.4:</b> CO <sub>2</sub> P(GPU) and CO <sub>2</sub> /CH <sub>4</sub> Selectivity of Various HFM .....	26
<b>Table 3.1</b> Membrane Sample Compositions.....	30
<b>Table 5.1:</b> UTS Results for different membrane samples.....	40
<b>Table 5.2:</b> Gas Permeation Results.....	43

## LIST OF ACRONYMS AND SYMBOLS

<b>CA</b>	Cellulose acetate
<b>CTA</b>	Cellulose Triacetate
<b>PSf</b>	Polysulfone
<b>HFM</b>	Hollow fiber membranes
<b>CO<sub>2</sub></b>	Carbon dioxide
<b>H<sub>2</sub>S</b>	Hydrogen sulfide
<b>CH<sub>4</sub></b>	Methane
<b>TW</b>	Terawatt-hour =10 <sup>9</sup> kW
<b>GT</b>	Gigatons
<b>Bcm</b>	Billion cubic meter
<b>SEM</b>	Scanning electron microscopy
<b>AFM</b>	Atomic force microscopy
<b>NMP</b>	N-methyl-2-pyrrolidone
<b>XRD</b>	X-ray Diffraction
<b>UTM</b>	Universal Testing Machine
<b>UTS</b>	Ultimate Tensile Strength
<b>FTIR</b>	Fourier Transform Infrared Spectroscopy
<b>NG</b>	Natural Gas

## ABSTRACT

Natural gas is one of the most abundant fuel resources in the world, combustion of which fulfils much of our energy needs. However, the presence of certain, noncombustible, and hazardous impurities may reduce the energy content of the fuel gas. CO<sub>2</sub> has adverse effects in this regard. It is mainly present in the order of 3-4% in natural gas, and increased amount reduces energy content of the gas. Therefore, it is imperative to separate carbon dioxide. The escalating demand for clean and sustainable energy sources has intensified research efforts towards efficient separation techniques for mitigating carbon dioxide (CO<sub>2</sub>) emissions. This thesis explores the fabrication and permeation analysis of Polysulfone modified Cellulose Triacetate blend membranes designed for the separation of carbon dioxide (CO<sub>2</sub>) from methane (CH<sub>4</sub>). The initial section of this thesis presents a thorough analysis of the current energy landscape, highlighting the importance of CO<sub>2</sub> separation technologies in the context of environmental conservation and sustainable energy consumption. Pristine and blend CTA/PSf membranes were synthesized from a solution of the polymers in N-Methyl-2-pyrrolidone. These membrane samples were then analyzed for gas permeation using single permeation testing (in PHILOS® Type) gas permeation equipment, also analyzed their surface characteristics studied and morphology using SEM analysis, for their tensile strength using the UTM, and the presence of different functional groups was confirmed using FTIR spectroscopy. It was found that the CTA/PSf membranes gave much better and superior single gas selectivity of 30.70 for the membranes containing 6wt% PSf in the CTA matrix, with permeabilities up to 11.12 Barrers. Moreover, they had a maximum tensile strength of about 18.51 MPa. In conclusion, this thesis advances the field of CO<sub>2</sub> separation by presenting a systematic exploration of PSf modified CTA blend membranes as a viable solution for efficiently removing CO<sub>2</sub> from CH<sub>4</sub>.

**Keywords:** Polymer blend membranes, Cellulose triacetate, Polysulfone, Methane purification (CO<sub>2</sub>/CH<sub>4</sub>), Global warming · CO<sub>2</sub> capture.

# CHAPTER 1: INTRODUCTION

## 1.1 Background

Due to industrial manufacturing of commodities to suit the demands of the global community, energy consumption is quickly rising as the world's population continues to expand. Energy is needed for the increased industrial production. Petroleum derivatives including combustible gas, coal, and lubricants account for around 64% of the world's power energy needs. Due to their finite reserves and rapid depletion, fossil fuels cause problems for the economy and ecology. Resource depletion and climate change brought on using fossil fuels have made it clear that switching to another energy system is required. [1]

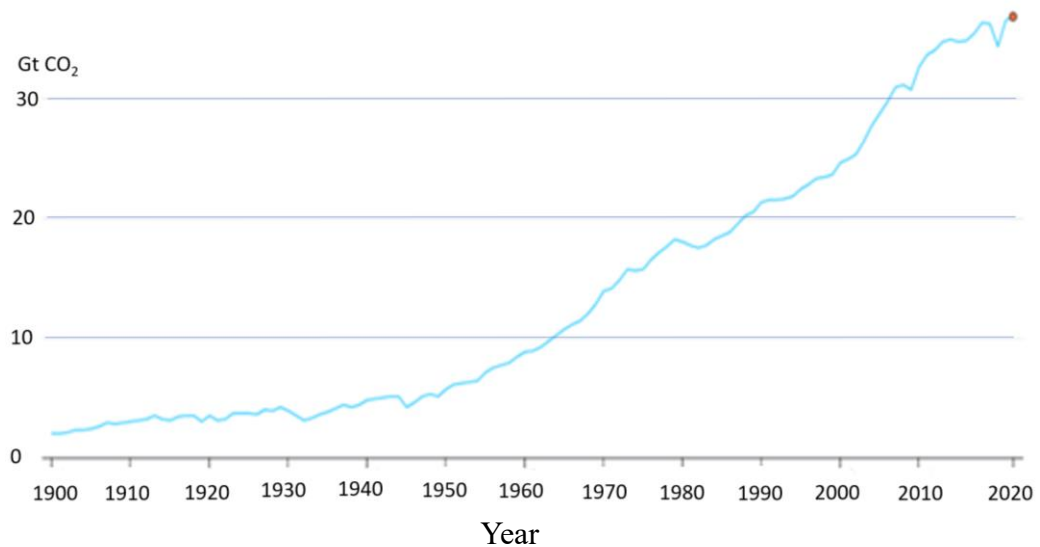


**Figure 1.1:** CO<sub>2</sub> Emissions from combustion of fuel and industrial activities, 1900-2022

During the industrial revolution, the amount of CO<sub>2</sub> in the atmosphere has increased significantly over the last 200 years. Total global greenhouse gas emissions ascended from 34.1 Gt in 2010 to 37.9 Gt in 2019, reported by the European Union's Joint Research Centre. The COVID-19 epidemic and associated transit and travel limitations decreased greenhouse gas emissions to 35.962 Gt in 2020, but emissions are projected to rise again once totals for 2021 are available. China was the world's top CO<sub>2</sub> emitter in 2020, with 11.680 Gt, or 32% of total worldwide emissions. The United States was close behind, generating 4.535 Gt, accounting for around 12.6% of global greenhouse gas emissions. Please keep in mind that these calculations are based on



data accessible through September 2021, and that actual values may change. Figure 1.1 illustrates the increment of CO<sub>2</sub> emission from 1900 to 2022. However, the outlook for the fossil fuel energy system is not encouraging. Their reserves have already reached their maximum levels. The US Department of Energy has anticipated that coal, natural gas, and oil will last 100, 150, and 50 years, respectively. There are no fresh reserves being found. The prediction for the global energy usage rate, however, is not a positive one because it assumes that by the end of 2050, demand would have practically doubled. [1], [2]

The global energy consumption of individuals is about 13 TW as shown in figure 1.2 the total contribution of different sources used for power generation. The electricity generation based on fossil fuels was “set to cover 45% of additional demand in 2021 and 40% in 2022 and coal-fired electricity generation to rise “by almost 5% in 2021 and a further 3% in 2022, after having declined by 4.6% in 2020. To meet the increasing demand for energy globally and maintain a low level of atmospheric CO<sub>2</sub> concentration. By the middle of the century, at least 10 TW of carbon-free energy should be generated. According to Hoffert et al., it will need the production of 15, 25, and 30 TW of carbon-free energy to keep the atmospheric CO<sub>2</sub> concentration at 550, 450 and 350 ppm, respectively, by 2050.

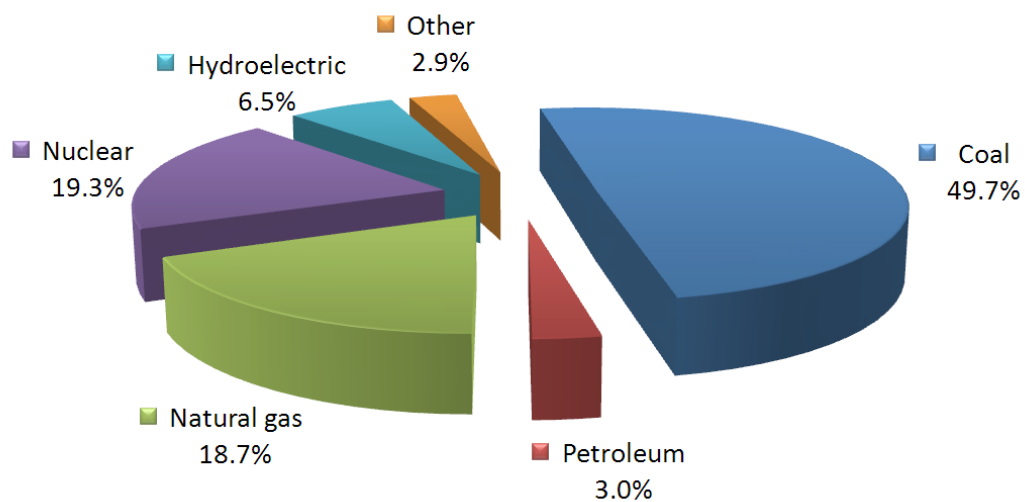


**Figure 1.2:** Percentage contribution of different sources used for power generation.

In a different estimate conducted in 2000 for 14 EU countries, the relationship between energy consumption and population was examined, and Table 1.1 illustrates the pattern that showed population growth and energy consumption rose concurrently.

**Table 1.1:** Correlation between population (in thousands) and energy consumption (in thousands of metric tons of oil equivalent)[3]

<b>Year</b>	<b>Population</b>	<b>Energy Consumption (TW)</b>
2000	376,037	1,460,284
2025 – Lower	374,902	1,805,297
2025 – Medium	393,659	1,953,477
2025 – Higher	412,144	2,101,007

Thus, a growth in population necessitates an increase in energy production, which calls for an increase in fuel supplies. Because the gasoline we now have is already running out very quickly. According to studies done by N.A. Owen et al., oil reserves increased in the early 1900s, particularly from 1930 onwards. But, after 1972, the oil supplies began to run out. This indicates that more oil was extracted from the reservoirs than was discovered there. Around 1980, the reserves were steadily running out, which showed that there were less conventional energy supplies available. As we've already shown, adding CO<sub>2</sub> lowers the energy output of fuel gases. So, if we want to enhance the output from traditional energy sources, we must lower the CO<sub>2</sub> content of the natural gas being utilized.

## **1.2 Consumption of Natural Gas**

The use of natural gas (NG) is the cleanest, finest, and most effective source of energy worldwide. When consumed, it emits between 26% and 41% less carbon dioxide than both coal and oil, respectively. Heavy gaseous hydrocarbons, acid gases, vapors of water, mercury, radioactive gases, and other gases such as nitrogen and helium are also present in varying quantities. The exact makeup of a typical raw NG is demonstrated in Table 1.2. The chemical composition of NG varies with geography. This table shows the composition derived for Canada (Alberta), New Mexico (Rio

Arriba County), Nigeria (Eleme), Southwest Kansas, Texas (Cliffside Field, Amarilla), Tunisia (Miskar), Vietnam (Bach Ho), and other countries. [3], [4]

**Table 1.2:** Typical Natural gas Composition[4]

<b>Components</b>	<b>Composition Range (mol%)</b>
Helium (He)	0.0-1.8
Nitrogen (N <sub>2</sub> )	0.21-26.10
Carbon Dioxide (CO <sub>2</sub> )	0.06-42.66
Hydrogen sulfide (H <sub>2</sub> S)	0.0-3.3
Methane (CH <sub>4</sub> )	29.98-90.12
Ethane (C <sub>2</sub> H <sub>6</sub> )	0.55-14.22
Propane (C <sub>3</sub> H <sub>8</sub> )	0.23-12.54
Butanes (C <sub>4</sub> H <sub>10</sub> )	0.14-8.12
Pentanes and Heavier	0.037-3.0

The global consumption of natural gas is anticipated to experience a minor contraction in 2022, followed by constrained expansion over the subsequent three years. This would result in a total increase of about 140 billion cubic meters between 2021 and 2025. This rise is much lower than the impressive 370 bcm increase seen in the previous five-year period, and it falls well short of the extraordinary jump in demand forecast for 2021, which is estimated to reach about 175 bcm as depicted in figure 1.3. The Asia Pacific area and industrial production continue to be the principal drivers of this increase, accounting for 50% and 60% of total expansion through 2025,

respectively. However, it is vital to highlight that both variables are vulnerable to possible price increases and drops in economic development.

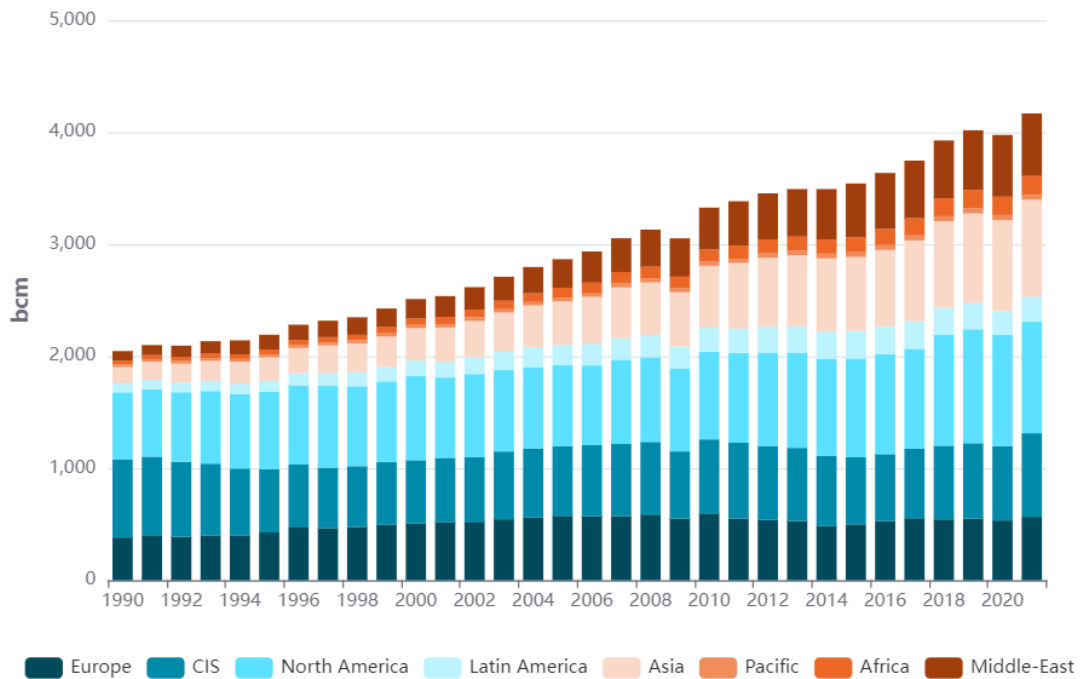


**Figure 1.3:** Natural Gas Consumption around the world [1]

### 1.3 Requirement of CO<sub>2</sub> Separation from Natural Gas

Eliminating acidic CO<sub>2</sub> from natural gas is critical not just for environmental reasons (emission reduction), but also for retaining the heating value of the gas and protecting pipeline integrity from corrosion. To meet pipeline criteria, CO<sub>2</sub> content must be reduced to less than 2%[5].

### 1.4 Techniques used for the Refinement of NG

Absorber and stripper units are essential components in the **h-BN** removal process from natural gas. These units rely on high-pressure absorber towers that are designed to handle fluctuating CO<sub>2</sub> levels. Larger towers are required to successfully handle increasing amounts of natural gas. The absorbent fluid in these towers is critical in absorbing CO<sub>2</sub> from the gas stream.

Despite its effectiveness, there is a trade-off: around 10-20% of the incoming gas is used in the absorption process, resulting in a reduction in overall useable gas production. However, the major benefits gained surpass this tradeoff, including the

capacity to satisfy demanding pipeline requirements and reduce the environmental effect of CO<sub>2</sub> emissions. In essence, absorber, and stripper units, along with their related high-pressure absorber towers and absorbent fluids, are critical for improving natural gas quality while matching sustainability goals.[4]

#### *1.4.1 Pressure Swing Absorption*

PSA is based on the structural and functional characteristics of adsorbent materials, which under high pressure generated a stronger physical connection with the adsorbate impurities. The removal of contaminants from input streams involves the use of a variety of materials. Table 1.3 lists several adsorbents and their corresponding adsorbing impurities. Large, fixed beds in the shape of cylinders make up the PS unit. Under high partial pressure, the contaminants from reactors are absorbed inside these beds. While adsorbents are being renewed, these pollutants are then discharged from the beds at low pressure. The PSA process consists of five basic phases in general[6].

1. Process of adsorption
2. Process of Re-pressurization
3. Process of Counter-current depressurization
4. Process of Purging
5. Process of Co Current depressurization

In PSA, process, high pressure feed gas containing impurities is introduced, and these impurities are subsequently confined inside the beds, resulting in high purity hydrogen at the product sides. To provide a continuous flow of feed and product, several adsorber are employed in parallel and series. Fresh adsorbers are provided with feed gas each time. These contaminants begin to saturate the adsorber. The adsorber is simultaneously depressurized during the second stage to remove the last of the hydrogen that was trapped inside the adsorber beds during the first step. During the countercurrent depressurization process, the adsorber underwent partial regeneration to remove the contaminants. The beds are fully restored in the fourth phase by removing the hydrogen that was purged in the second step. The feed stream repressurized the adsorber together with some of the product and hydrogen taken from the second stage to keep the adsorber at the proper pressure. The cycle is then repeated by starting a process. the 200kPa-or-less hydrogen collected from the product side.

Recompression after transit and transportation requires additional energy. Hence, this approach is not appealing for the filtration of gases.

**Table 1.3:** Materials used for pressure swing Adsorption

Adsorbent materials	Adsorbates
Gel Silica	CO <sub>2</sub> , H <sub>2</sub> O, Hydrocarbons
Activated Carbons	CO <sub>2</sub> , Methane, Nitrogen
Molecular Sieving (Zeolites)	Methane, CO <sub>2</sub> , Nitrogen
Alumina oxides	Water
Carbon Molecular Sieving	Oxygen

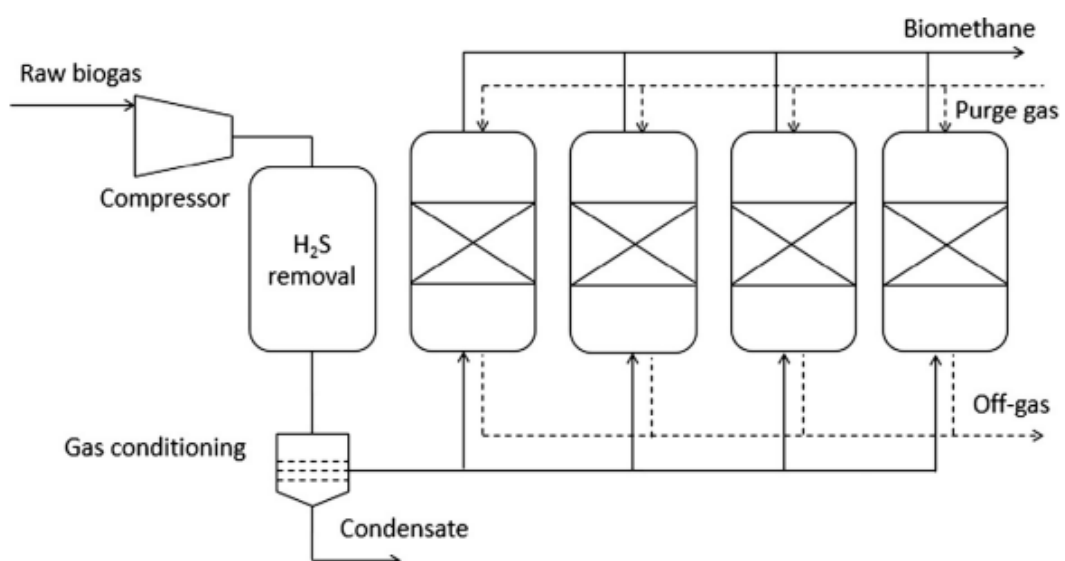


**Figure 1.4:** Process Flow Diagram of PSA Process

### 1.4.2 Cryogenic Distillation

The boiling points difference of the input gas streams was used in cryogenic distillation. It is a commercially accessible low temperature process. The ability of the procedure to create liquid hydrogen that is ready for shipment is its main benefit. Moreover, no chemical reagents are employed in this procedure. Compared to other acidic gases, hydrogen has a substantially lower boiling point. Hydrogen must be liquefied using a high-energy refrigeration system since its boiling point is substantially lower. The main limitations of the cryogenic process are the high capital and operating costs and process pore blockage. Cryogenic distillation is also not practical on a small scale.[6]

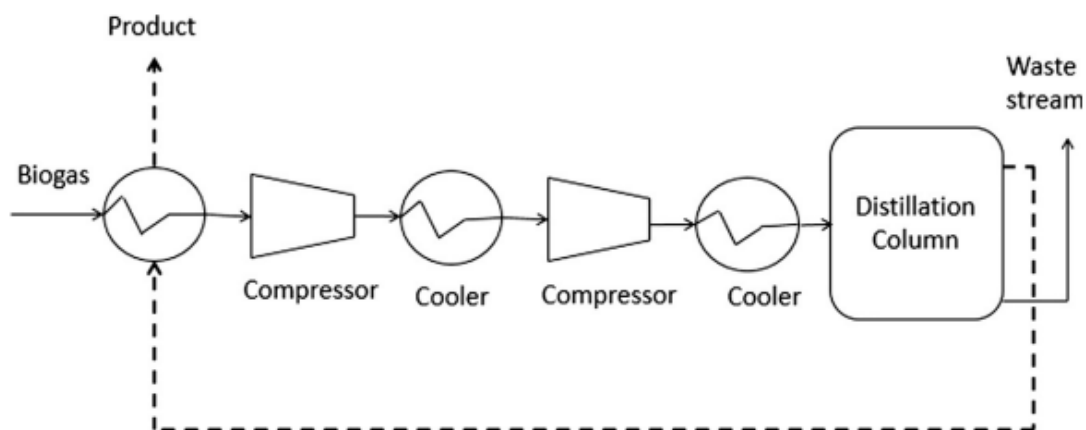


**Figure 1.5:** Process Flow Diagram of Cryogenic Distillation

### 1.4.3 Membrane Technology

Due to the fundamental characteristics of membrane operations—they do not involve transitions in phase or additions of chemicals, are simple in impression and functioning, they are flexible as well as simple to scale-up, and have the potential for more efficient use of raw materials—membrane-based natural gas advancement represents an intriguing alternate to traditional upgrading technologies like absorption and cryogenic distillation. The large footprint of offshore projects, which is a major restriction, makes the rising towers of the amine absorber unit (Figure 1.6) problematic. Therefore, numerous gas oil firms still view membrane technology as a promising treatment option for natural gas. Membrane modules for gas permeation and membrane contactors are essentially 2 distinct membrane techniques that can be utilized to separate  $\text{CH}_4$  from  $\text{CO}_2$ [7].

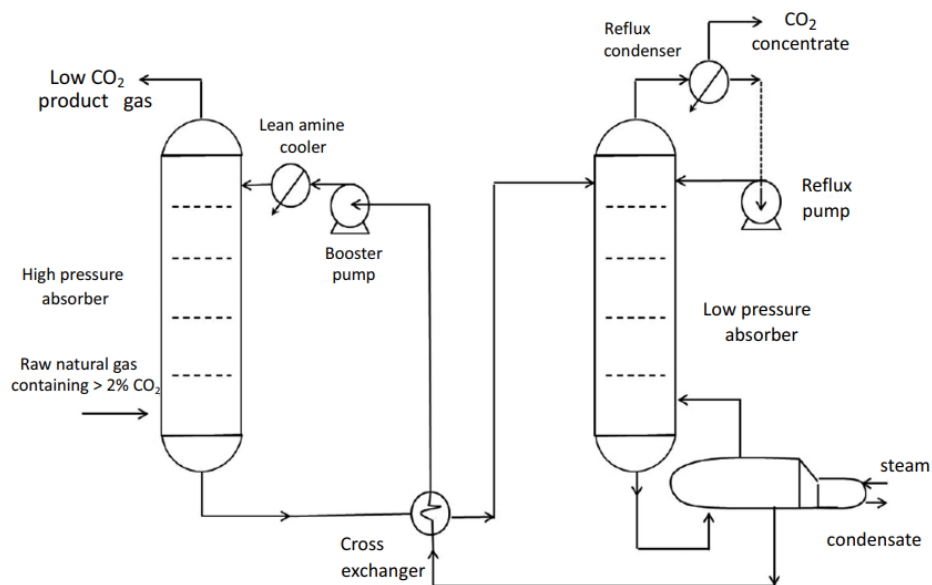


**Figure 1.6:** Amine Sweetening PFD

A thinner selective membrane is used in the gas permeation membrane process to separate a mixture of gases into two streams, the permeating stream comprised of a more permeable gas and the retentate being rich in the gas retained. The membrane modules utilized in the CO<sub>2</sub>/CH<sub>4</sub> separation scenario are made of crystalline polymers, with Carbon dioxide being more permeable than methane and splitting the desired gas, CH<sub>4</sub>, direct at elevated pressure by the retentate stream (Figure 1.7).

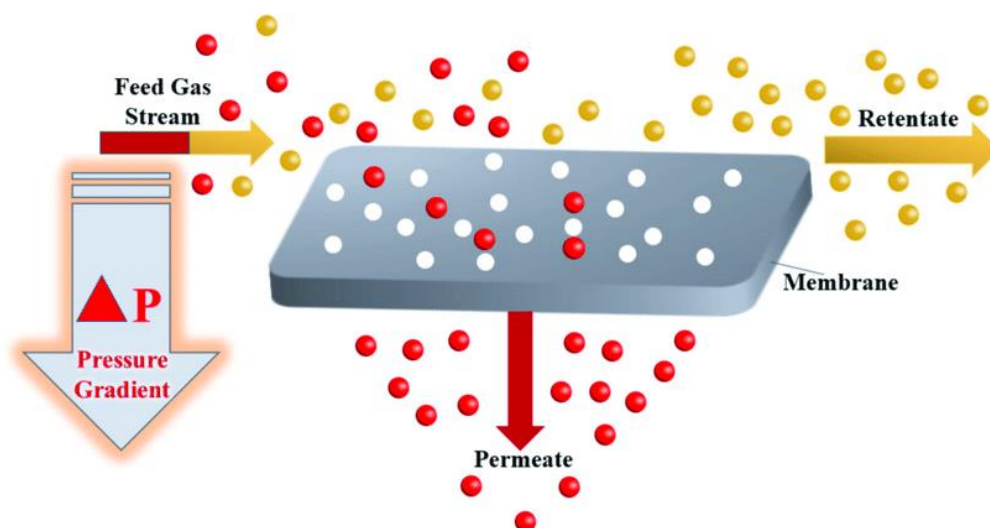


**Figure 1.7:** Gas penetration across a membrane

The permeabilities of the given gas component and the optimal selectivities of the membranes are the most significant aspects of membrane gas separation.



Permeabilities, or gas transfer, is an important characteristic of dense polymer membranes and is determined using equation (1):

$$J = \frac{D_i K_i \Delta P}{l} \quad (1)$$

The interaction between permeability and selectivity lies at the heart of efficient membrane-based gas separation systems.  $J_i$  (measured in  $\text{cm}^3$  (STP)/ $\text{cm}^2$  s) denotes the gas component flow, where " $l$ " represents the membrane thickness.  $P$  denotes the difference in partial pressures of component " $i$ " upstream and downstream.  $D_i$  represents the diffusion coefficient of component " $i$ " in the membrane material, whereas  $K_i$  represents the gas sorption coefficient in the same material.  $P_i$ , the product of  $D_i$  and  $K_i$ , represents membrane permeability, which assesses the membrane's ability to allow gas passage. The membrane selectivity ( $i/j$ ) for two gases, " $i$ " and " $j$ ," is defined as the ratio of their permeabilities (2) and serves as a measure of the membrane's efficacy in separating the two gases.[6]–[8]

$$\alpha = \frac{P_i}{P_j} = \left[ \frac{D_i}{D_j} \right] \times \left[ \frac{K_i}{K_j} \right] \quad (2)$$

The notion of  $[D_i/D_j]$  is introduced in Equation (2), which indicates the ratio of diffusion coefficients for components  $i$  and  $j$ , indicating diffusivity or mobility selectivity. Furthermore, the solubility selectivity is defined as the ratio of solubility coefficients, represented as  $K_i/K_j$ . This equation shows how selectivity variables affect separation efficiency in the context of gas diffusion over membranes.

Monsanto Prism pioneered industrial membrane technology for gas separation using polysulfone-based membranes in 1977, with the goal of regulating the  $\text{CO}_2/\text{H}_2$  ratio of syngas for a petrochemical process. In 1978, a crucial step was taken when a membrane separation system was developed to recover hydrogen from an ammonia purge gas stream. This novel technique represented a significant leap in membrane-based gas separation. Similarly, the system was used to separate nitrogen from methane and carbon dioxide, demonstrating its adaptability and broadening its applicability to diverse gas separation procedures. Later, Dow commercialized glassy polymeric membranes. Then, in the 1980s, Cynara and UOP Separex Membrane Technology commercialized carbon dioxide removal from natural gas. GKSS/MTR has more recently begun to sell membranes for  $\text{CO}_2$  separation. Due to their low cost and ease

of production, polymeric membranes are currently used commercially for CO<sub>2</sub> extraction methods[9]. However, the stability, selectivity, and permeability of these compounds are generally low. The membranes are said to plasticize under high CO<sub>2</sub> pressures, for example, and the materials age, which are two signs of low stability. Refer to Table 2.1 for information on commercial polymeric membranes developed for CO<sub>2</sub> extraction from CH<sub>4</sub>. A solution-diffusion process is responsible for mass transfer via these thick polymeric membranes. This method produces mixture selectivity values that are often less than 50, as well as permeance values that are normally in the range of 5 to 10<sup>-9</sup> mol/m<sup>2</sup>sPa.

## 1.5 Motivation

The global demand for clean and sustainable energy sources has become increasingly urgent in current years, membranes separation has appeared as a promising resolution for selective CO<sub>2</sub> removal from various gas streams, particularly in the field of CO<sub>2</sub>/CH<sub>4</sub> separation. We are interested in learning more about blended membranes comprising a combination of two different polymers of tailored properties, the impacts of CO<sub>2</sub> passage through the membranes of different compositions.

However, there are still significant challenges in order to achieve high CO<sub>2</sub> selectivity, permeance, and long-term stability. Therefore, this thesis aims to explore the fabrication techniques and analyze the performance of blended membranes for CO<sub>2</sub>/CH<sub>4</sub> separation, advancements in fabricated membrane was done by using different weight % of polysulfone polymer in a fixed amount of cellulose triacetate polymer matrix.

Also, it lessens the negative effects of different solvents on the environment, and the effects of CO<sub>2</sub> presence in natural gas stream.

## 1.6 Objective

The objective of this research work is as follows:

- (1).Fabrication of pristine and Blended Cellulose triacetate and Polysulfone membranes.
- (2).Characterization and Permeation analysis of fabricated membrane samples.
- (3).Optimization of membranes as a function of blend percentage/ composition.

Finally, we intended to do a comparison study of blended membranes and pure CTA and PSf membranes in terms of separation performance, and also recommended future advancements based on the comparison's findings.

## CHAPTER 2: LITERATURE REVIEW

Carbon dioxide, a non-combustible gas, must be removed from natural gas extracted from reservoirs because it affects the overall energy content of the gas reserves. There are several membranes utilized for this purpose, however polymer blend membranes and mixed matrix membranes are the most discussed issues among researchers.

### 2.1 Membrane Materials

The permeability (productivity) and selectivity (efficiency) of the membrane customized for a particular gas separation job are the two main criteria that receive the most attention in the field of membrane-based gas separations. To achieve higher degrees of permeability and selectivity, many membrane materials have been investigated. These materials may be roughly divided into polymeric, inorganic, mixed matrix, and blended membranes.

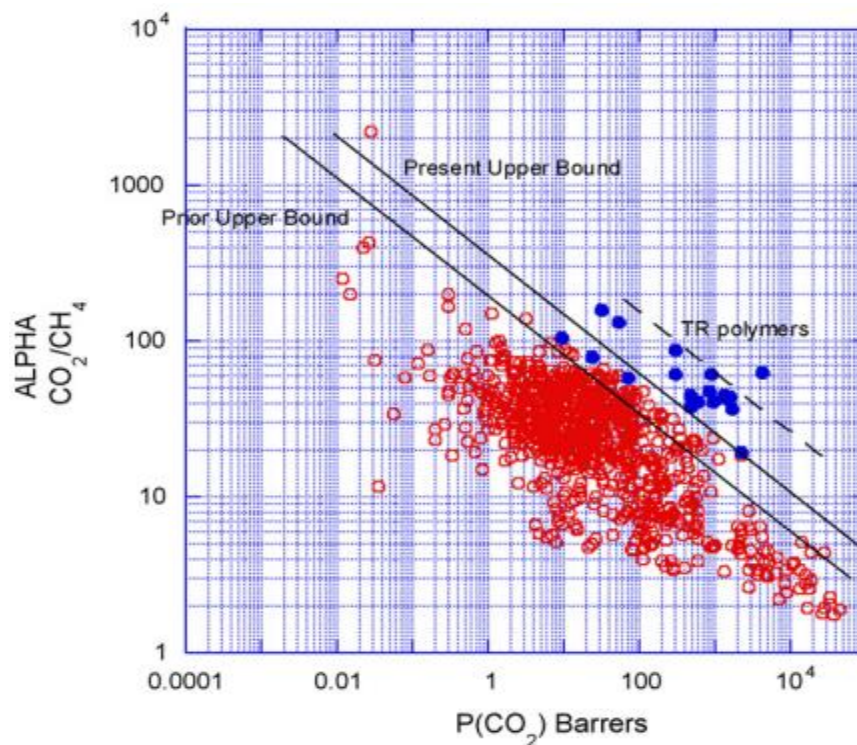


**Figure 2.1:** Robeson plot for gas pair (CO<sub>2</sub>/CH<sub>4</sub>) Separation [10].

Selecting the appropriate membrane material improves permeability ratios and helps achieve superior permeability performance. The type of separation sought

determines the choice of membrane chemistry, which is equally important. Therefore, choosing the best membrane material is of utmost importance. Notably, the application of the membrane in industrial settings is further strengthened by an asymmetric membrane arrangement[10].

### *2.1.1 Polymeric Membranes*

Organic materials including cellulose triacetate (CTA), polysulfone (PSf), polyimide (PI) polycarbonate (PC), and polydimethylsiloxane (PDMS), are utilized to make many commercially accessible membranes, which are polymeric and constructed of these materials. Membranes with aforementioned materials, are simple to manufacture, offer a high level of selective as well as permeability, and are very strong mechanically. Testing polyvinyl amine/polyvinyl alcohol mix membrane led to a total of 98% CH<sub>4</sub> purity. The first commercially available membrane for gas purification was the Cellulose acetate membrane, which eliminates CO<sub>2</sub> and H<sub>2</sub>S. Due to the outstanding separation qualities of cellulose, which is a renewable and abundant material, cellulose acetate is cheap. Because it has a few restrictions, the application of Cellulose Acetate membranes in gas separation is limited. Due to plasticization events, the CA membrane displayed a poorer gas mixture selectivity than the selectivity that is estimated for pristine gas. due to the -OH functional group, which makes it easier for CO<sub>2</sub> to dissolve in the membrane matrix, makes it vulnerable to plasticization (plasticization = 8 bar). Due to the greater permeability of gas being achieved as compared to other synthetic polymers, PDMS (polydimethylsiloxane) was thought to be an exceptional option. Because of the wide variety of configurations and the nature of the side chain, PDMS has a comparatively higher permeability of CH<sub>4</sub> and CO<sub>2</sub> than other materials. Low separation factor and low mechanical strength are two clear drawbacks of this type of material.[6], [11]

In the context of separating H<sub>2</sub>S and CO<sub>2</sub> from natural gas, modern polymeric membranes have gained economic competitiveness when juxtaposed with conventional technologies in terms of both operational and capital costs. The subsequent Table 2.1 enumerates commercial membrane materials alongside their selectivity for eliminating impurities from natural gas. Despite the promising outcomes seen in gas separation, polymeric membranes are beset by substantial limitations. A significant challenge, as earlier indicated, pertains to their diminished selectivity,

necessitating a multi-stage separation setup that escalates capital expenditure. Additionally, polymeric membranes struggle to uphold performance under extreme environmental conditions characterized by high pressure and temperature, leading to their degradation. The presence of substantially corrosive elements in the supply causes chain swelling, which is the principal cause of these problematic events. Compaction, membrane aging, and plasticization are other concerns.

**Table 2.1:** Commercially used membrane material for impurity removal from natural gas.

<b>Polymer</b>	<b>Material Category</b>	<b>Permeated Gases</b>	<b>Selectivity CH<sub>4</sub> with different Gases</b>
Ether-amid block co-polymer	Rubbery	Hydrogen Sulfide	20-30
Polyimide, CA, Perfluoro polymer	Crystalline	Carbon dioxide	10-20
Silicon Rubber	Rubbery	Nitrogen	0-3
perfluoro polymer	Crystalline	Carbon dioxide	2-3
Silicon Rubber	Rubbery	Higher hydrocarbon	5-20

Membranes with high permeability frequently have poor selectivity for certain gas combinations. The following Table 2.2 lists many advantages and disadvantages of polymer membranes.

**Table 2.2:** Characteristics, cons, and types of polymer membranes

Characteristics	<ol style="list-style-type: none"><li>1. Polymers exhibit flexibility and softness in their rubbery state, transitioning to hardness and rigidity in the glassy state.</li><li>2. Glassy membranes demonstrate elevated glass transition temperatures (T) compared to rubbery counterparts, resulting in higher CO<sub>2</sub>/CH<sub>4</sub> selectivity.</li></ol>
Disadvantages	<ol style="list-style-type: none"><li>1. Handling carbon dioxide may provide plasticization issues.</li><li>2. When exposed to CO, the polymer network swells and has higher segmental mobility, resulting in improved gas permeability.</li><li>3. Because gases with originally limited permeability may undergo increasing penetration, this phenomenon might result in decreased membrane selectivity.</li></ol>
Examples	Cellulose Acetate (CA), Polyether Amide (PEA), Poly-sulfone (PSf), Polydimethylsiloxane (PDMS), Polyethylene, Poly-imide (PI) Poly-ether sulfone (PES),

### 2.1.2 In-Organic Membranes

In-organic membranes provide multiple advantages over traditional polymeric membranes, most notably improved heat stability, chemical resistance, and mechanical robustness. As a result, they are a better choice. These membranes are commonly made from carbon molecular sieves (CMS), zeolites, metal-organic frameworks (MOFs), and ceramics. Inorganic membranes outperform polymeric equivalents in terms of

selectivity and gas flow rates. CMS and zeolites, for example, outperform polymeric membranes in terms of selectivity and diffusivity.[5]

Inorganic membranes provide multiple advantages, including solvent resistance at high pressures and high-temperature stability (Table 2.3). whereas, inorganic membranes have several limitations as well, such as expensive fabrication and operational costs, a low surface area per unit volume, and difficulty transforming them into large surface area modules for industrial usage.[12]

The heightened selectivity observed in these membranes can be attributed to their precise capacity for distinguishing shapes and sizes, resulting in a narrower range of pore sizes. Importantly, as illustrated in Figure 2.1, many inorganic membranes surpass the Robeson upper limit by effectively combining both selectivity and permeability.

**Table 2.3:** Pros and Cons of inorganic membranes

<b>Advantages</b>	<b>Disadvantages</b>
Robustness under elevated pressure conditions	Brittleness is a weakness.
Ability to withstand significant pressure differentials	Increased operational costs
Economic viability in operational aspects	The difficulties in establishing significant selectivity for large-scale micro-porous membranes
Endurance against adverse environmental impacts	Elevated Temperature complex membranes to module sealing
Simplified and efficient cleaning procedures	Permeabilities of substantial selective thick inorganic membranes is reduced at moderate temperatures.



## 2.2 Mixed Matric Membranes

Extensive research work has been steered to overcome issues to in cooperate inorganic and polymeric membranes encounter. These materials' shortcomings pushed researchers to innovate and create a new membrane substance with enhanced mechanical resilience, excellent separation performance, and cost-effectiveness. This resulted in the advancement of (MMM) mixed matrix membranes, which merge inorganic and organic materials. The goal of this innovation was to improve gas separation efficiency without incurring expensive costs. MMM fabrication has gained popularity as a preferred method because it not only improves mechanical properties but also combines the more separation capabilities and stability inherent in in-organic components through the competent processability of polymeric membrane materials. In the world of MMM, inorganic fillers are methodically placed inside the polymer matrix, whether solid, liquid, or a mix of both. This strategic component integration enables MMM to capitalize on the pros of increased selectivities provided by disperse fillers while balancing them with the improved processability and mechanical robustness inherent in polymers. The diagram in Figure 2.2 below depicts the pinnacle of MMM's ideal structure[13].

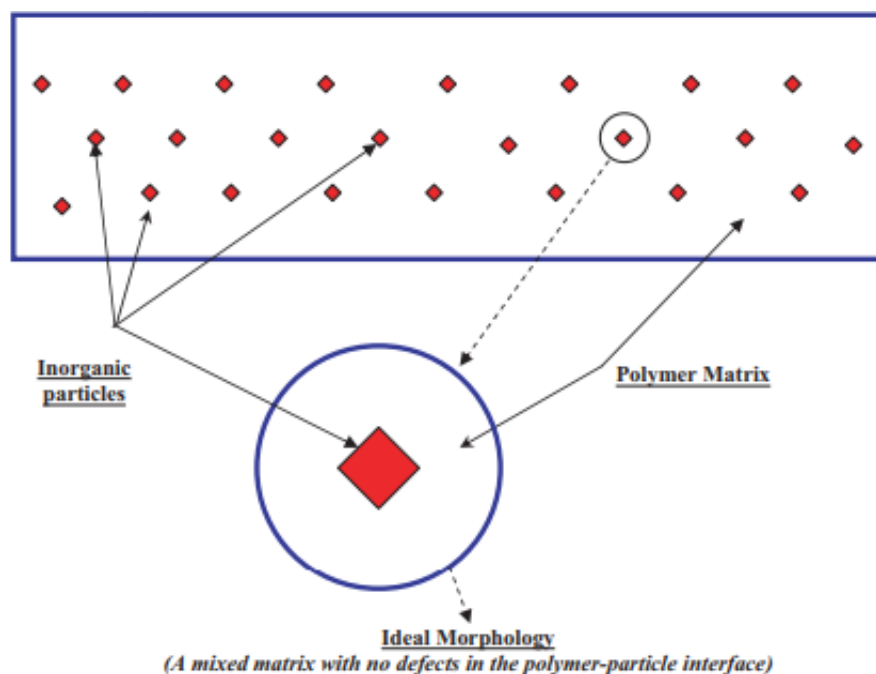


**Figure 2.2:** Schematic diagram of an ideal MMM

The continuous polymeric matrix is delineated by the unshaded zone in the figure 2.2, while the dispersed phase (fillers) is marked by tiny, stippled squares.

### 2.2.1 *Fillers for Mixed Matrix Membranes (MMM)*

Mixed matrix membranes, abbreviated as MMMs, consist of a polymeric matrix blended with dispersed filler particles. Within MMMs, these fillers hold a pivotal role in elevating membrane properties and performance. It's noteworthy that the selection of the appropriate filler hinges on the intended application and the specific attributes sought in the mixed matrix membrane. Diverse fillers possess the capacity to introduce distinct functionalities and advantages to the resulting MMM, ultimately enhancing its performance across a range of applications, such as gas separation, water treatment, and various membrane-based separation processes[14]

Here are some different types of fillers commonly used in mixed matrix membranes:

#### 2.2.1.1 Inorganic Fillers

Due to their advantageous attributes, including a substantial surface area, robust tensile strength, and compatibility with polymer matrices, zeolite and silica nanoparticles, or materials based on silica, are commonly utilized as additives in membrane technology. Recent research has highlighted the potential for zeolites to significantly enhance the permeability and selectivity of polymeric materials, contingent upon the specific zeolite-polymer pairing. Notably, three prominent zeolites in Mixed Matrix Membranes (MMMs) are ZSM-5, zeolite A, and zeolite Y. Additionally, Zeolites 13X and 4A have demonstrated their capacity to enhance the performance of zeolite-infused polymeric membranes, particularly in applications such as hydrogen-nitrogen ( $H_2/N_2$ ), carbon dioxide-nitrogen ( $CO_2/N_2$ ), and carbon dioxide-oxygen ( $CO_2/O_2$ ) separation. It's crucial to recognize that the gas permeability across a zeolite-infused polymeric membrane hinges on the inherent characteristics of both the zeolite and the polymer, as well as their interplay and the quantity of zeolite incorporated into the mixed matrix membrane [6], [13].

In a study by Kusworo et al., the introduction of 25% zeolite 13X into a PI/PES membrane resulted in a notable increase in  $CO_2$  permeability, rising from 6.54 to 15.04 Barrer, and an enhancement in  $CO_2/CH_4$  selectivity from 33.6 to 38.7 compared to the

pristine membrane. Another noteworthy zeolite, Zeolite Socony Mobil-5 (ZSM-5), has gained attention in MMM development [15]. Musselman and colleagues observed a remarkable enhancement when 30% ZSM-5 was incorporated into a Matrimid polymer matrix, leading to an increase in CO<sub>2</sub> permeability from 7.3 to 14.6 Barrer and an enhancement in CO<sub>2</sub>/CH<sub>4</sub> selectivity from 34.7 to 56.4 [16].

Amooghin et al. recently found that adding 15% nano-porous NaY zeolite to an incorporating 30% ZSM-5 into a Matrimid-based polymer matrix resulted in a notable 20% increase in CO<sub>2</sub> permeability.[17]. In contrast, Zhang et al. reported that introducing ZSM-5 into the Matrimid phase significantly increased CO<sub>2</sub>/CH<sub>4</sub> ideal selectivity to 67.2, exceeding the 34.7 CO<sub>2</sub>/CH<sub>4</sub> selectivity of pure Matrimid. Furthermore, in binary gas separation (75% CO<sub>2</sub>, 25% CH<sub>4</sub>), a greater CO<sub>2</sub>/CH<sub>4</sub> selectivity of 67.4 was attained[18]. Tantekin-Ersolmaz et al. studied the effect of zeolite particle size on zeolite-PDMS MMMs, stating that bigger zeolite particles increased permeability while showing less variance in selectivity.[19]

#### 2.2.1.2 Metal oxides:

Metal oxide nanoparticles, including titanium dioxide (TiO<sub>2</sub>) and zinc oxide (ZnO), have the capability to enhance the performance of MMMs by providing improved selectivity and stability. TiO<sub>2</sub> particles with the particle size of 3nm were used as a filler over the Matrimid 5218 by Moghadam et al. to create the MMMs using the solution casting technique[20]. Additionally, they noticed that agglomeration was seen at high volume fractions of TiO<sub>2</sub>, whereas the spreading of the filler in mixed matrix membranes was more regular at minimal volume fractions over Matrimid 5218. TiO<sub>2</sub> was added to Matrimid, and it was determined that this membrane performance. The inclusion of filler also decreased its elongation percentage and tensile strength. In contrast to the pristine polymeric membrane, the permeability of CO<sub>2</sub> was enhanced by up to 1.86 times. At a filler amount of 25wt% of filler content. MMMs were created by Liang et al. for gas separation. As a filling, spherical-shaped TiO<sub>2</sub> nanoparticles (NPs) with surface area of 19.7m<sup>2</sup>g<sup>-1</sup> and an average particle size of 70nm were used. To separate CO<sub>2</sub> from CH<sub>4</sub>, these NPs were added to polyether sulfone (PES). To evaluate how the filler affects the selectivity and porosity of Mixed Matrix Membranes (MMM), various weight percentages (2%, 4%, 10%, and 20%) of TiO<sub>2</sub> filler were introduced into a PES matrix.

The findings demonstrated that MMMs with high filler content experienced significant issues like agglomeration because of the weak adhesion between PES and TiO<sub>2</sub>. The filler and polymer matrix's various polarities would be the cause of the poor adhesion. TiO<sub>2</sub> and the polymer substrate (PES) both displayed hydrophobic and hydrophilic properties. Both the filler (TiO<sub>2</sub>) and the polymer substrate (PES) exhibited hydrophobic and hydrophilic properties in nature, respectively. The selectivity of the membrane was raised from 24.5 to 34 using 4 weight percent of TiO<sub>2</sub>. Additionally, selectivity decreased as the filler material increased. As shown in figure 2.3, on the other hand, increasing the weight percentage of TiO<sub>2</sub> filler improved the permeability of MMMs[21].

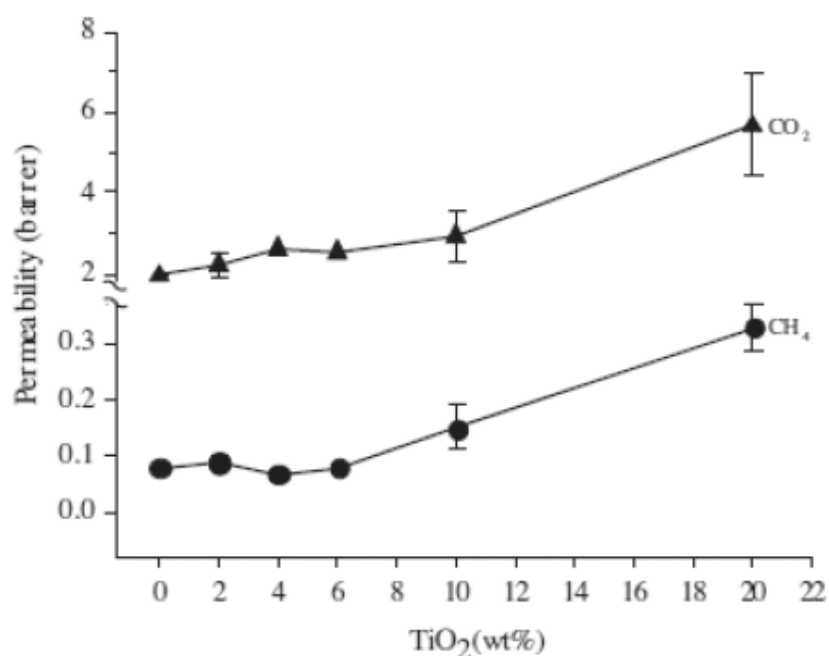


**Figure 2.3:** Gas Permeability of CO<sub>2</sub> from different wt% of TiO<sub>2</sub>

MMMs were created by Hu et al. to separate CO<sub>2</sub> from CO<sub>2</sub>/CH<sub>4</sub> gas mixture. The fluorinated polyamide was filled with TiO<sub>2</sub> to enhance the separation efficiency of MMMs. With the addition of TiO<sub>2</sub>, the traditional membrane becomes rigid and denser, increase in selectivity from 29.3 to 33.3, was seen. In the case of CO<sub>2</sub>, permeability was also observed to be reduced[22].

### 2.2.1.3 Ionic Liquid Mixed Matrix Membranes

Benjamin Lam et al. studied how IL doping affects CTA-based membrane properties for CO<sub>2</sub>/CH<sub>4</sub> separation. [emim][BF<sub>4</sub>] and [emim][dca] ILs were chosen for

their selectivity. IL doping's impact on polymer characteristics, gas solubility, permeability, and CO<sub>2</sub>/N<sub>2</sub> separation was assessed, offering a fresh approach to enhance CTA's CO<sub>2</sub> removal from CH<sub>4</sub> and N<sub>2</sub> mixtures[23].

Hamid Reza Mahdavi et al. studied Pebax1074-based membranes, enhancing gas permeation with [BMIM] ionic liquids and Silicon dioxide nanoparticles. Ionic liquid gel membrane (ILGM) showed notable increases in carbon dioxide and methane permeabilities (from 2.9 to 104.3 Barer, and 5.6 to 58.6 Barer, respectively) with IL content rise, causing a slight decrease in CO<sub>2</sub>/CH<sub>4</sub> selectivity (from 20.2 to 18.5). Improved performance toward Robeson upper bound was evident, especially with 80 wt.% [BMIM][PF6]. Introducing SiO<sub>2</sub> nanoparticles in nanocomposite ILGMs (NCILGMs) further elevated CO<sub>2</sub> and CH<sub>4</sub> permeabilities (to 153.6 and 8.1 Barrer) and ideal selectivity (to 19.1). The optimum performance was observed in NCILGM containing 8 wt.% SiO<sub>2</sub>. Characterization encompassed XRD, ATR-FTIR, and FESEM analyses[24].

M. Bhattacharya et al. studied a mixed matrix membranes combining [EMIM][EtSO<sub>4</sub>] ionic liquid with PEBA elastomer for H<sub>2</sub>S and CO<sub>2</sub> separation. The 5 wt% IL content increased H<sub>2</sub>S permeability (540 Barrer) and reduced CO<sub>2</sub> permeability (55 Barrer) at 7 kg/cm<sup>2</sup> pressure. Permeability trend: H<sub>2</sub>S > CO<sub>2</sub> > Air > CH<sub>4</sub>. High ideal selectivity for H<sub>2</sub>S/CH<sub>4</sub> (66.0) and H<sub>2</sub>S/Air (24.0) versus CO<sub>2</sub>/CH<sub>4</sub> (4.6) and CO<sub>2</sub>/Air (2.4). IL improved acid gas permeability over pure PEBA membranes[25].

#### 2.2.1.4 Metal-organic frameworks (MOFs):

MOFs are structured crystalline materials comprising metal ions and organic ligands. These materials have features such as a large surface area, tunable pore sizes, and superior adsorption characteristics, which can lead to better gas separation.

P. Tanvidkar et al. created a cellulose acetate membrane in their investigation. With cost in mind, the produced Mixed Matrix Membranes (MMMs) were tested for gas separation performance at reduced feed pressures (1.5, 2 bar). MMMs with 5 and 10% ZIF-8/CA had the highest results, with CO<sub>2</sub> permeabilities of 9.65 and 9.5 Barrer, respectively, which were almost twice those of pure CA. Furthermore, the CO<sub>2</sub>/CH<sub>4</sub> selectivity was determined to be 10.37 and 15.3 for these compositions. The

permeabilities exceeded the model predictions when experimental data were compared to projected gas permeation results utilizing MMM transport models[26].

### 2.3 Blend Membranes

For this reason, polymer blends are used, as polymer blends are an impressive technique for use in gas separation and have many advantages over mixed matrix and inorganic membranes. These advantages include simple design, easy fabrication, and concerted effect of the blending components of a membrane. The utilization of miscible blends has been a longstanding practice in the realm of gas separation.

The effect of Polyethylene glycol concentration on gas permeabilities and selectivity in blend membranes was examined by Li et al. They developed miscible mixtures with varied PEG weights (200, 600, 2000, and 6000) and PEG 20,000 concentrations (10-60 wt%). The 10% PEG 20,000 mix membranes outperformed others in CO, N<sub>2</sub>, and CH<sub>4</sub> permeability tests at 30-80°C and 20-76 cmHg, indicating better CO<sub>2</sub> permeability and CO<sub>2</sub>/CH<sub>4</sub>, CO<sub>2</sub>/N<sub>2</sub>, selectivity. CO<sub>2</sub> permeabilities exceeded 200 barrer at 70°C and 20 cmHg, and selectivity reached 22. PEG 20,000 mixes exhibited higher diffusivity coefficients, which improved CO<sub>2</sub> permeability even though CO<sub>2</sub>/CH<sub>4</sub> selectivity was lower than CA membranes from 30 to 80°C[27].

MMMs for gas separation were invented by A.R. Moghadassi et al. They employed [CA/PEG/MWCNTs] and [CA/SBR/MWCNTs] versions of cellulose acetate (CA) blends with multi-walled carbon nanotubes (MWCNTs), both raw and functionalized (C-MWCNTs). Tetrahydrofuran (THF) solution casting was used to construct membranes. C-MWCNTs increased performance, increasing selectivity (CO<sub>2</sub>/CH<sub>4</sub> and CO<sub>2</sub>/N<sub>2</sub>) from 13.41 to 21.81 and from 9.33 to 13.74 at 0.65 wt% MWCNTs, respectively. PEG and SBR effects were investigated; at 2 bar pressure, [CA/PEG/C-MWCNT] obtained 53.98 CO<sub>2</sub>/CH<sub>4</sub> selectivity and [CA/SBR/C-MWCNT] achieved 43.91. Pressure increased permeability and selectivity. Mechanical characteristics improved as MW-CNTs, and polymer mixing were increased[28].

Chunhai Yi et al. explored the impact of blending poly(vinylamine) and polyethylene glycol on membrane structure and the performance of CO<sub>2</sub>/CH<sub>4</sub> separation. The experiment indicated that the crystallinity of the membrane diminishes

as the poly (ethylene glycol) (PEG) concentration increases, resulting in greater penetration rates for both CO<sub>2</sub> and CH<sub>4</sub>. The mix membrane containing 10% PEG performed best, with the greatest pure carbon dioxide penetration rate of 5.8106 cm<sup>3</sup> (STP)/cm<sup>2</sup> s cmHg and achieved a maximum selectivity of 63.1 at a temperature of 25°C and a feed pressure of 96 cm Hg. The research also delved into the consequences of cross-linking and the interplay between CO<sub>2</sub> and CH<sub>4</sub>. Particularly, membrane cross-linking boosted selectivity considerably. An unexpected coupling effect was identified while evaluating mixed gases with a constant CH<sub>4</sub> partial pressure but variable CO<sub>2</sub> partial pressure: when CO<sub>2</sub> partial pressure increased, CH<sub>4</sub> permeation rate increased. This coupling process adds to increased selectivity[29].

A. Car et al.'s research focuses on developing a specialized polymeric membrane from multi-block copolymers, particularly, copolymers like poly (ethylene oxide)-poly (butylene terephthalate) offer the ability to finely adjust their attributes by modifying both the PEO phase fraction and molecular weight. These structural modifications have a discernible impact on the transport properties of four gases: carbon dioxide, hydrogen, nitrogen, and methane are carefully investigated. Following characterization, the two most promising copolymers are selected to create tailored blends using polyethylene glycol. The top-performing co-polymer, including 55 wt% of 4000 g/mol polyethylene oxide, produces a very high CO<sub>2</sub> permeability of 190 barer, more than two times of the pure copolymer. [30] Simultaneously, the selectivity between CO<sub>2</sub> and H<sub>2</sub> is improving. Findings imply that geomorphology of PEO-PBT copolymers may accurately regulated by inserting lower molecular wt of PEG, resulting in adjustable gas transportation characteristics.

Cai et al. also created a miscible membrane by mixing polyallylamine (PAAm) and polyvinyl alcohol (PVA) as the solvent. These membranes had a CO<sub>2</sub>/N<sub>2</sub> selectivity around 80 and CO<sub>2</sub>/CH<sub>4</sub> selectivity = 58. Aside from miscible blend membranes, there is another type known as immiscible blend membranes. Extensive study is now being conducted in this sector, with multiple papers addressing the subject[31].

Numerous investigations, notably the work of Kapandaitakis et al., have looked into this topic. They demonstrated a hybrid membrane made of poly-sulfone (PSf) and polyimide (PI), with the goal of studying gas separation and penetration capabilities for both individual gases and gas combinations. Permeability values for gases like Helium, Hydrogen, Nitrogen, and Oxygen, which have no chemical interaction with

polymeric components, were comparable to those of pure PSf and pure PI. However, gases that interact with the components, such as CO<sub>2</sub>, revealed permeability variations that could not be described purely by simple mixing formulae. Surprisingly, the study discovered that raising the PSf level in the membrane reduces the plasticization impact of CO<sub>2</sub>. This feature qualifies the membrane for high-pressure applications as well as scenarios involving carbon dioxide-rich streams. The study also found that selectivity changed with PSf quantity, with selectivity ranges of 6-7 for O<sub>2</sub>/N<sub>2</sub>, 25-30 for CO<sub>2</sub>/N<sub>2</sub>, and 3-5 for H<sub>2</sub>/CO<sub>2</sub> [32].

Wang et al. created an immiscible blend membrane employing two separate polyether sulfone (PES) grades: Victrex 4800P and Radel A-300. These were dissolved in a solvent solution that included N-methyl-2-pyrrolidone (NMP) and a variety of alcohols (methanol, ethanol, 1-propanol, 1-butanol, 1-pentanol, ethylene glycol, and diethylene glycol). The membranes produced have a maximum He/N<sub>2</sub> selectivity of around 4.58[33].

J. Li et al. created blend membranes of cellulose acetate (CA) and polyethylene glycol (PEG) utilizing a dichloromethane and tetrahydrofuran solvent system. The CA membrane containing 10% PEG and having a molecular weight (MW) of 20000 had the maximum selectivity. The selectivities for CO<sub>2</sub>/N<sub>2</sub> and CO<sub>2</sub>/CH<sub>4</sub> were measured to be 36.2 and 30.3, respectively. After assessing the benefits of integrating amine groups into the structure and analyzing several instances of both miscible and immiscible blends, it was found that employing a mix membrane of cellulose acetate and polyallylamine may be a viable alternative. This method provides the advantages of amine group addition while making use of the availability of cellulose acetate, making it a realistic option.

## **2.4 Membrane Modules**

Kim et al. created hollow fiber membranes out of TR poly-benzoxazole (TR-PBO). Asymmetric hollow fiber membranes were generated initially from a hydroxyl poly (amid acid) precursor and subsequently exposed to temperatures over 400°C, resulting in TR-PBO hollow fiber membranes. Surprisingly, the skin structure and porosity substructure were preserved even after heating above the glass transition temperature (T<sub>g</sub>) of the precursor polymers. These TR polymer membranes performed exceptionally well in gas separation, particularly in CO<sub>2</sub> separation, without exhibiting



substantial plasticization effects. This is crucial since alternative gas separation membranes frequently suffer problems with CO<sub>2</sub> absorption and subsequent plasticization under high-pressure circumstances. TR polymers offer a viable answer to this problem. Table 2.4 displays permeance and selectivity statistics for a variety of hollow fiber membranes made of polyimide, polysulfone, and other materials. Those formed from 6-FDA-durene display good thermal and mechanical qualities, as well as remarkable gas separation capability, making them appropriate for a wide range of industrial applications[34].

**Table 2.4:** CO<sub>2</sub> P(GPU) and CO<sub>2</sub>/CH<sub>4</sub> Selectivity of Various HFM

HFM	P (atm)	T (°C)	Permeance (CO <sub>2</sub> ) (GPU)	Permeance (CH <sub>4</sub> ) (GPU)	Selectivity (CO <sub>2</sub> /CH <sub>4</sub> )	Type of Gas	
6-FDA-2,6-DAT	13	20	58.8	1.41	41	Mixed	[35]
6-FDA-2,6-DAT/1% (w/v)	2.5	20	24.7	0.41	59	Mixed	[35]
TR-PBO	1.5	-	1932.8	136.9	17	Pure	[34]
6-FDA-durene	2.5	30	372	18	19.6	Pure	[35]

Chung et al. found that the CO<sub>2</sub> permeance was 373 GPU (Gas Permeation Units), which they ascribed to enhanced molecular chain packing caused by shear stress caused by the interaction of 6-FDA-durene polyimide with CO<sub>2</sub>. Furthermore, the TR-PBO membrane module had the greatest CO<sub>2</sub> permeance, outperforming the other modules by over 1,000 GPU. This excellent performance was accomplished by lowering the membrane's skin layer thickness, demonstrating the potential of TR-PBO in improving gas permeance[35].

Because all pristine polymeric membranes were fully developed and could no longer provide exceptional strength, permeability, and selectivity, alternative modules and mixed matrix membranes were created.

## CHAPTER 3: MATERIALS AND METHODS

### 3.1 Materials Utilized

Polymers Cellulose triacetate (CTA) with 2.84 degree of acetylation, Polysulfone (PSf) with Molecular weight of 22,000 were bought from Aldrich Sigma, N-methyl-2-pyrrolidone (NMP) solvent were utilized for membrane fabrication also purchased from Aldrich Sigma. Figures 3.1 and 3.2 show the chemical compositions of the polymers utilized. Whereas high purity Carbon dioxide and Methane gases were supplied by Paradise company, Pakistan.

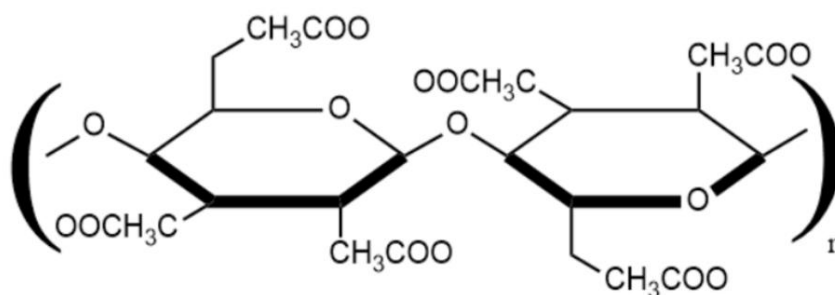


**Figure 3.1:** Cellulose-triacetate Structure[36]

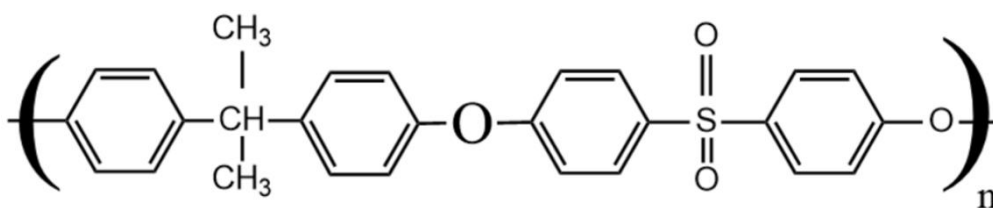


**Figure 3.2:** Polysulfone Structure[37]

### 3.2 Membrane Fabrication

#### 3.2.1 Pristine and Blend Membranes Fabrication

In the synthesis of pristine and blend membrane, a 10 wt/vol % solution of cellulose triacetate (CTA) and polysulfone (PSf) polymers is prepared using the solution casting technique, resulting in the formation of a membrane with desirable

properties. Initially, the polymers Cellulose triacetate (CTA), and beads of polysulfone (PSf) polymer were both kept in vacuum drying oven at 65°C for the removal of moisture, then 1gm of cellulose triacetate is dissolved in 10ml N-methyl-2-pyrrolidone (NMP), to create a 10 (w/v) CTA solution [39]. Simultaneously, polysulfone, a high-performance thermoplastic polymer known for its chemical resistance and mechanical strength, is dissolved in N-methyl-2-pyrrolidone (NMP) as solvent[40]. The two polymer solutions are then mixed in pre-determined ratios, ensuring thorough homogenization. This blending process enables the combination of desirable characteristics from both polymers, including the hydrophilicity of cellulose triacetate and the robustness of polysulfone. The polymers solution was then stirred overnight. The resulting homogeneous blend solution was poured to a clean glass plate and allowed to evaporate slowly at room temperature or under controlled conditions. To ensure the complete removal of solvent cast polymer solution underwent heat treatment at 95°C for 4-5 h. As the solvent evaporates, the polymer chains progressively self-assemble and solidify, resulting in the formation of a continuous thin film. Finally, the blended membrane sample is carefully peeled off the petri dish, washed with a suitable non-solvent to eliminate any remaining casting solvent, and then dried, resulting in a defect-free, synthesized blend membrane composed of 10wt% cellulose triacetate and polysulfone polymers[38], [40].

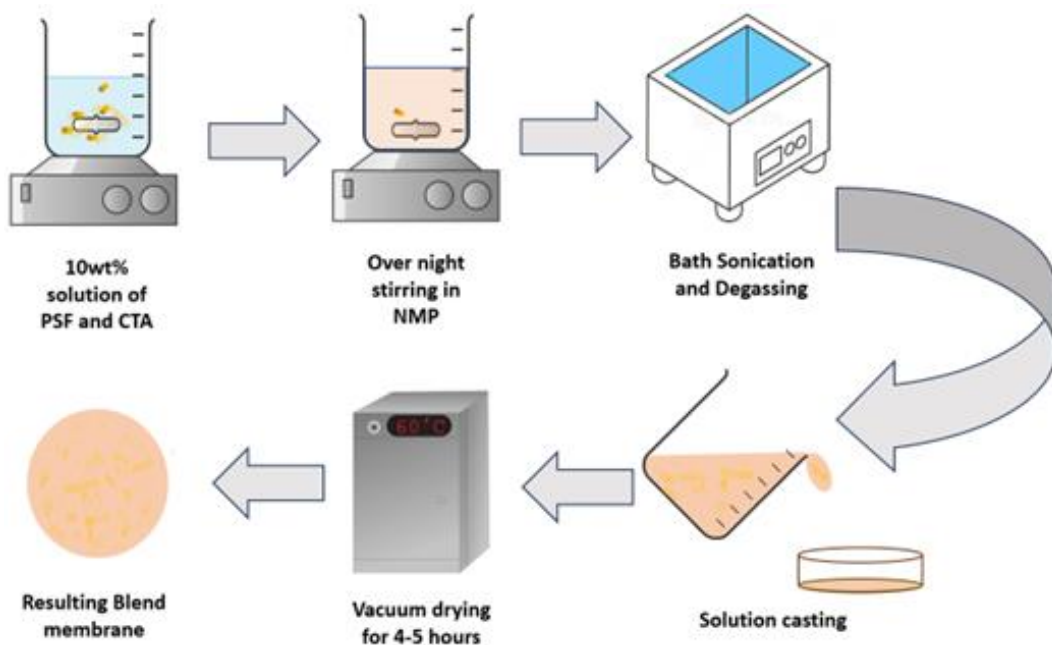


**Figure 3.3:** Fabrication of CTA/PSf Blend Membranes

Table 3.1 below contains compositions of all the pristine and blended membrane samples.

**Table 3.1** Membrane Sample Compositions

<b>Samples</b>	<b>Polymer (A) Main matrix</b>	<b>Polymer (B)</b>	<b>Blend samples</b>
Sample 1	100% CTA	--	Pure CTA
Sample 2	--	100% PSf	Pure PSf
Sample 3	CTA	2% PSf	2 wt.% CTA/PSf
Sample 4	CTA	4% PSf	4 wt.% CTA/PSf
Sample 5	CTA	6% PSf	6 wt.% CTA/PSf
Sample 6	CTA	8% PSf	8 wt.% CTA/PSf
Sample 7	CTA	10% PSf	10 wt.% CTA/PSf

This blended membrane exhibits improved properties, such as enhanced mechanical strength, thermal stability, and increased resistance to chemical degradation, making it suitable for various applications, including filtration, separation, and purification processes. The resultant membranes were then used for gas permeation testing and characterization.

### **3.3 Gas Permeation**

The permeation test was performed on single gas using a (PHILOS® type) gas permeation equipment. All the measurements for gas permeations were performed at (25<sup>0</sup>C) room temperature, at different feed pressures of 2,3,4 and 5 bars, the pressure at the permeating side was kept constant i.e., 1 bar. Each sample of membrane was cut as per the size of porous support disk present in the membrane sample holder of equipment. To measure the volumetric flow (Q) rate of permeating gas, a bubble flow meter was coupled to the permeate side of membrane[41]. A flow diagram of

(PHILOS® type) gas permeation equipment is shown in the figure 3.4. Each composition of the membrane was tested three times for confirmation of the results and average values are reported in this work.

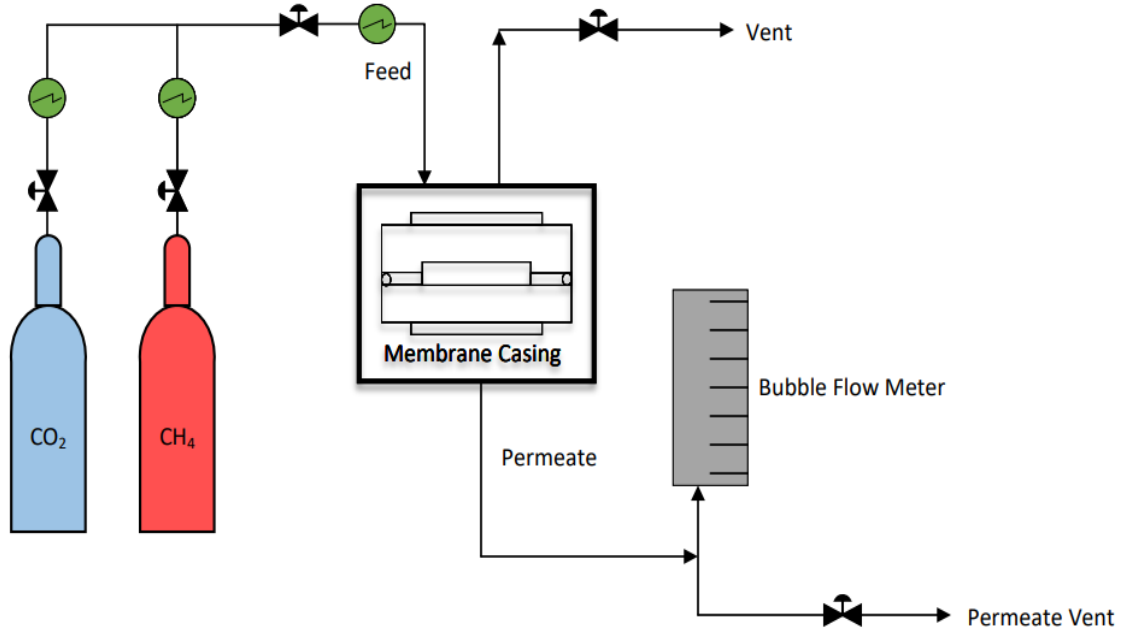


**Figure 3.4:** Permeation Equipment Flow Diagram

Permeabilities of gases were calculated using the following equation.

$$\frac{P_i}{\Delta l} = \frac{Q_i}{\Delta P * A} \quad (3) \quad [42]$$

Where, Permeability of respective gas in Barrer is represented as  $P_i$ . 1 Barrer =  $10^{-10} \text{ cm}^3 \text{ (STP) cm.cm}^{-2} \text{ s}^{-1} \text{ cm Hg}^{-1}$ .  $\Delta l$  is defined as average thickness of the membrane sample in cm.  $Q_i$  is volumetric flowrate ( $\text{cm}^3 \text{ (STP)/s}$ ).  $A$  and  $\Delta P$  are the effective area of the membrane ( $\text{cm}^2$ ), and the differential pressure in cm of Hg through the membrane respectively[42].

Also, the selectivity of CO<sub>2</sub>/CH<sub>4</sub> was calculated by using the quotient of permeabilities of CO<sub>2</sub> and CH<sub>4</sub> gas in a simple formula:

$$\alpha = P_{\text{CO}_2}/P_{\text{CH}_4} \quad (4) \quad [42]$$

Where,  $\alpha$  represents the ideal selectivity of CO<sub>2</sub>/CH<sub>4</sub>.

## CHAPTER 4: MEMBRANE CHARACTERIZATION

### 4.1 Fourier Transform Infrared Spectroscopy

The FTIR analysis of the fabricated membranes was carried out using a PerkinElmer Spectrum 100 Spectrometer, which is a widely used instrument for molecular characterization. The objective of this characterization technique was to identify, and to verify the presence of different functional groups, by the absorption of infrared radiation by the molecules within the membrane samples. The analysis was performed within  $4000\text{--}400\text{cm}^{-1}$  wavenumber range, encompassing the mid-infrared region. To facilitate the Fourier, Transform Infra-Red spectroscopy (FTIR) analysis, the fabricated membrane samples were subjected to meticulous cutting, to obtain representative sections for spectroscopic examination. By comparing the obtained spectra with established spectral libraries and known functional group vibrations, the presence and nature of various chemical groups within the membranes can be determined, providing valuable insights into their molecular composition and structural characteristics[43].

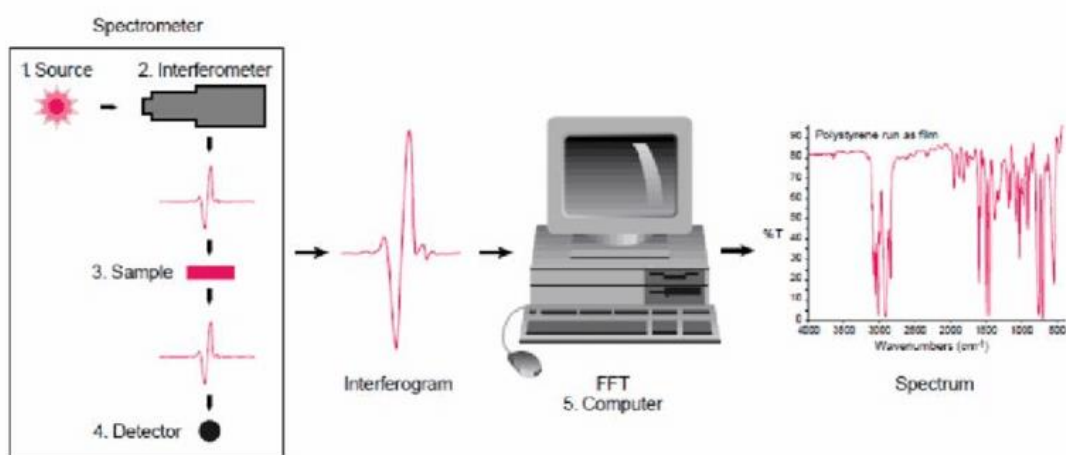


**Figure 4.1:** Working of Fourier Transform Infra-Red spectroscopy.

### 4.2 Scanning Electron Microscope

The SEM technique involves scanning a focused electron beam over the surface of the samples, generating high-resolution images that reveal surface topography, particle distribution, and pore characteristics. By assessing SEM micrographs obtained at different magnifications ranges, the porosity, morphology, and distribution of

polysulfone polymer within the Cellulose triacetate matrix can be assessed. By using the SEM and employing these specific settings, it became easier to analyze the physical characteristics of the membrane samples, such as their overall morphology, surface features, and the distribution of pores within the materials[43]. This information is essential for understanding the structural properties and potential applications of the membranes in fields such as filtration, separation, and other relevant areas.

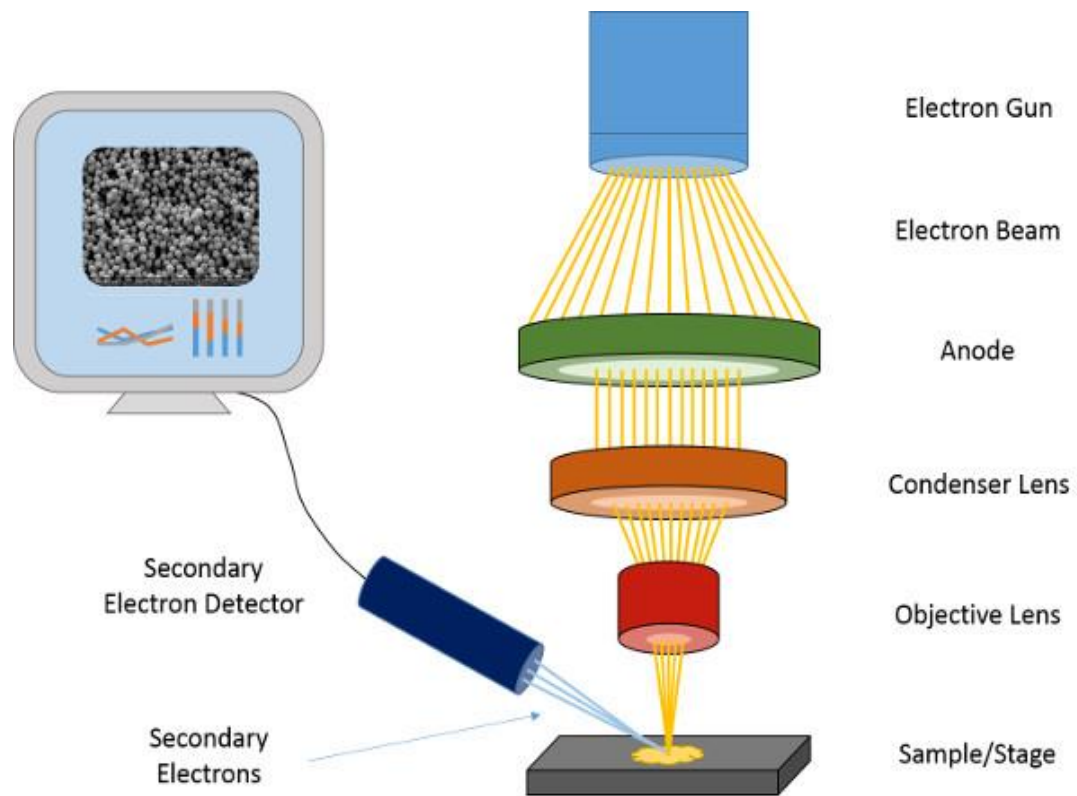


**Figure 4.2:** Scanning Electron Microscope Analysis

The morphology and pore distribution of fabricated membrane samples were investigated using the JEOL JSM-6490LA scanning electron microscope (SEM). The membrane samples were composed of cellulose triacetate (CTA) membrane matrix with varying concentrations of polysulfone (PSf) polymer[43]. The concentrations tested were 2wt%, 4wt%, 6wt%, and 8wt% of polysulfone in 1gm fixed amount of cellulose triacetate. An accelerating voltage of 15 kV was consistently employed during the imaging of all samples. Subsequently, the samples were magnified at different levels, including 500x, 1000x, 5000x, 10,000x, and 20,000x, to achieve higher resolutions and to examine the microstructural information in greater detail[44].



### 4.3 Ultimate Tensile Strength

The stress-strain behavior of the CA/PSf blend membrane samples containing 2wt%, 4wt%, 6wt%, and 8wt% was studied during the tensile test. This characterization method enables the determination of important mechanical properties such as ultimate tensile strength, which represents the maximum stress a material can withstand before fracture. By analyzing the stress-strain curves, the relationship between applied stress and strain deformation can be established[43].



**Figure 4.3:** Ultimate Tensile Strength Machine

Ultimate tensile strength was performed using a SHIMADZU AGSX series precision ultimate tensile tester, capable of exerting a maximum load of 50 kN. The samples under investigation, composed of CA/PSf blend membrane, were subjected to tensile testing according to the ASTM standard D882-02. The testing was conducted

at a strain rate of 0.5 mm/min, ensuring consistent and controlled deformation conditions[44].

#### 4.4 X-ray diffraction (XRD)

X-ray diffraction (XRD) analysis is a powerful, non-destructive, and highly versatile technique used to investigate the crystallinity of varied materials[43], [44]. It provides deep understanding of the atomic-level structure and composition of a wide range of materials, including minerals, metals, ceramics, and polymers, also, allows the identification of crystal orientations, crystalline phases, lattice parameters, and the presence of any structural defects or impurities. For the XRD analysis of membranes, samples were scanned from a  $2\theta$  value of 4–40[43].

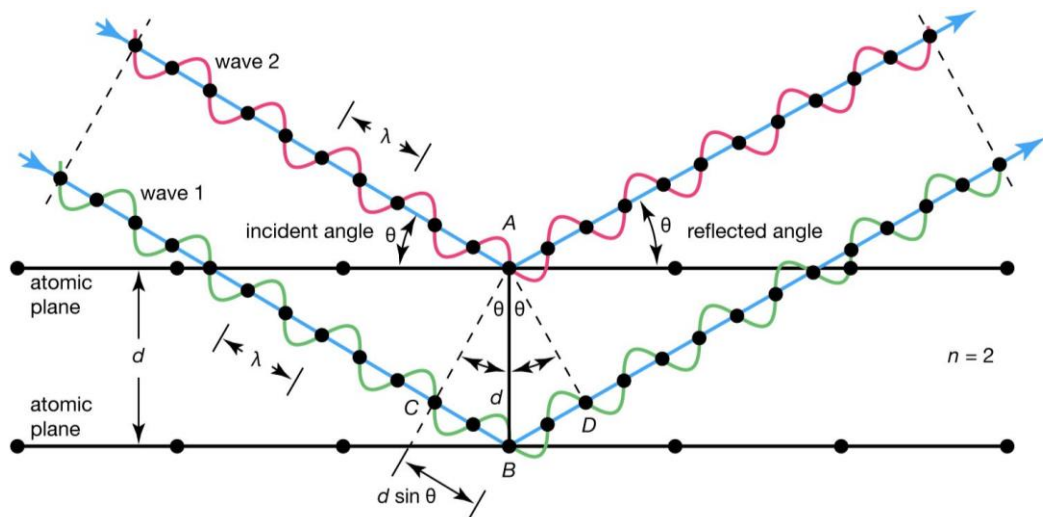


**Figure 4.4:** X-ray diffraction (XRD)

## CHAPTER 5 RESULT AND DISCUSSIONS

Fabricated membrane samples were characterized and examined by using different characterization techniques. The characterizations techniques which were used are as follows:

- FTIR was the technique used for the analysis of different functional groups present in the membrane matrix.
- XRD was used to investigate the crystallinity and the amorphous nature of the fabricated membrane samples.
- UTS was done to measure the mechanical strength and toughness of the membranes.
- SEM was used to evaluate the surface morphology and pore characteristics of the membrane.

### 5.1 FTIR Analysis

FTIR spectroscopy is an important technique which is used to characterize the important physical and chemical interactions occurring. Inverted bell-shaped peaks which appear in the FTIR spectrum represent the different functional groups present in the polymeric membrane matrix. Spectra of different pristine and blended membranes are illustrated in the Figure 5.1. A stretching around  $3750.50\text{cm}^{-1}$ - $3350.20\text{cm}^{-1}$  represents O-H bond, C-H bond stretching due to aliphatic and aromatic  $\text{Sp}^3$  hybridization was observed around region of  $2950.40\text{cm}^{-1}$ , after that stretching at  $1700\text{cm}^{-1}$ - $1750\text{cm}^{-1}$  will represent the presence of C=O in Cellulose triacetate[45], [46].

While the peaks around  $1250\text{cm}^{-1}$  and  $1360\text{cm}^{-1}$  represent C-O and  $\text{CH}_3$  (symmetric deformation), in cellulose triacetate[47], [48].

It is observed from FTIR result of pristine polysulfone (PSf) membranes that the stretching frequencies at  $2980\text{cm}^{-1}$ - $3150\text{cm}^{-1}$  was due to aliphatic and aromatic C-H bonds, sulfonated bond (S=O) symmetric and asymmetric vibrations were represented near region of  $1360\text{cm}^{-1}$ ,  $1163\text{cm}^{-1}$ . The benzene ring stretching and the aromatic C=C stretch was observed around  $1490\text{cm}^{-1}$  and  $1580\text{cm}^{-1}$ .

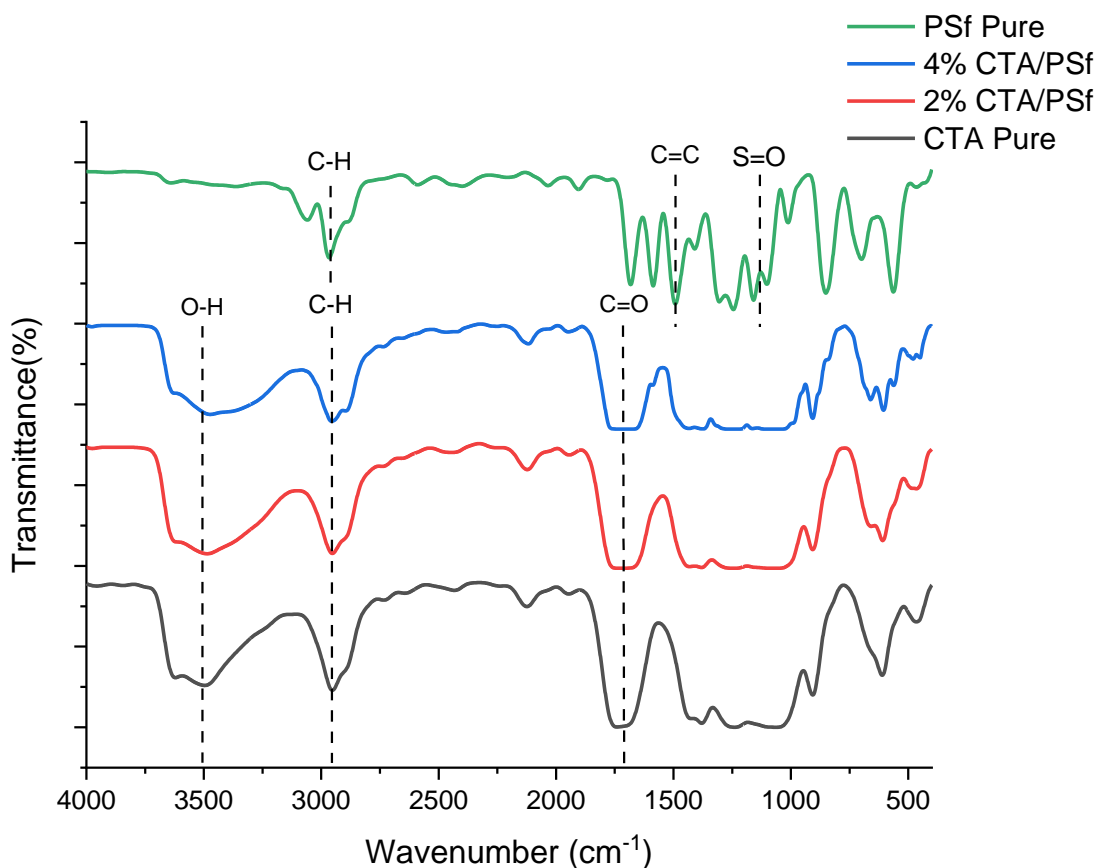


**Figure 5.1:** FTIR Results of Pristine CTA, PSf and CTA/PSf Blend Membranes

To check the miscibility of PSf and CTA C=C of benzene in FTIR results of CTA/PSf blended membrane of 2% and 4% CTA/PSf, was shown around  $1595\text{cm}^{-1}$ . The broad peaks around  $3752\text{-}3310\text{cm}^{-1}$  describe the O-H group additional no peaks were detected in blend membranes which confirms any other bond interaction[49].

## 5.2 XRD Analysis

Structural assessment of both the pristine and the polymer blended membranes of different weight percentages is performed using X-ray diffraction technique. The microstructure of polymer matrix contains both crystalline and amorphous regions. In the XRD spectrum, peaks with sharp and high intensities represent crystalline regions, whereas the broad and low intensified peaks represent the amorphous nature of the compound. Figure 5.2 illustrates the XRD patterns of all the fabricated samples. In the XRD spectrum of pure cellulose triacetate two major peaks at 2-theta values of  $8^\circ$  and  $19^\circ$ , which represents the crystalline and amorphous regions, respectively. On contrary pristine polysulfone XRD spectrum shows only one broad diffraction peak at  $2\theta$  value

of  $18^\circ$  which represents the semi crystalline nature of polysulfone (PSf) polymer as compared to the cellulose triacetate (CTA)[38], [45]. All the results and peaks were in good agreement with the literature. The XRD pattern of CTA/PSf blended membrane is shown in Figure 5.2.

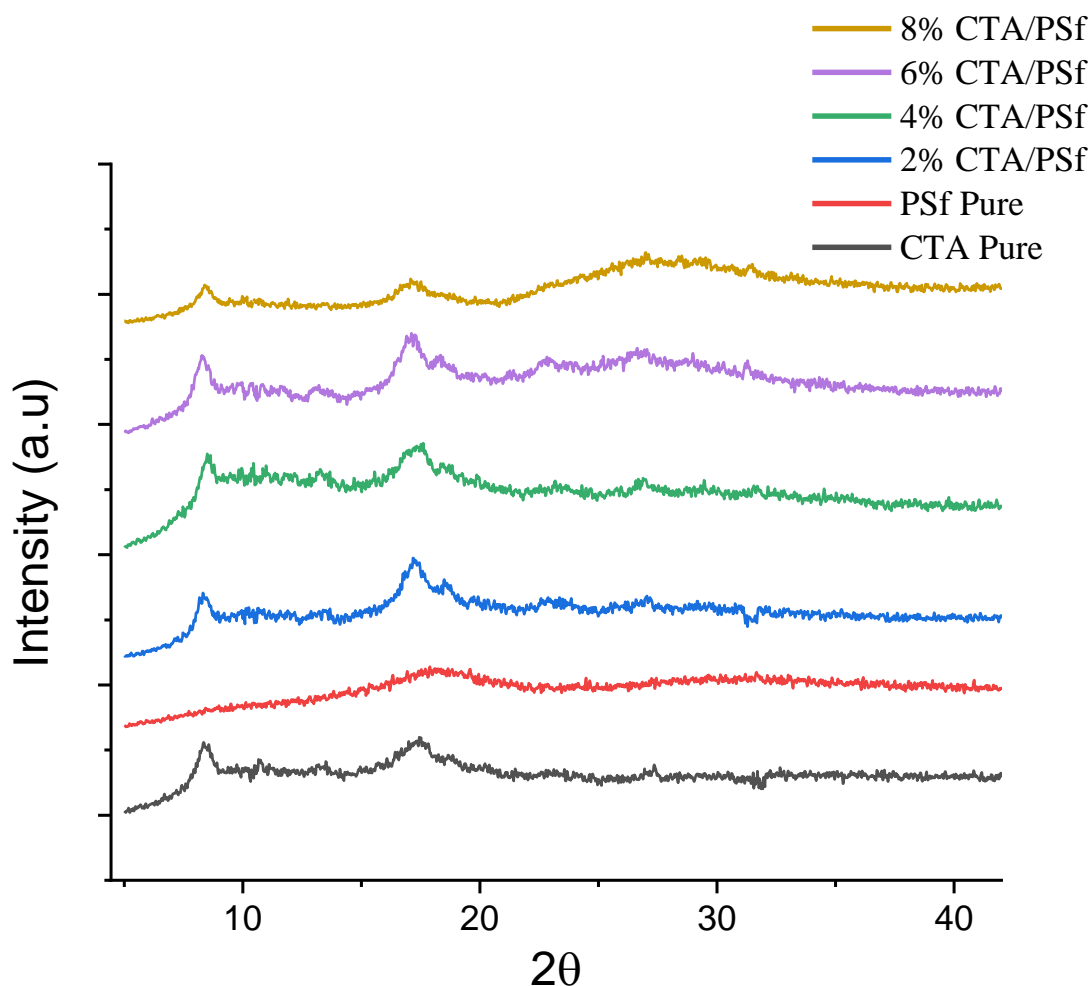


**Figure 5.2:** XRD Results of Pristine and CTA/PSf Blend Membranes

In the XRD spectrum of blend membrane samples initially no peak shift was observed, and no dominating peaks of polysulfone was shown which suggests that at lower loadings of PSf, the crystalline phase of cellulose triacetate is dominated, as PSf is relatively less crystalline or semi crystalline polymer in nature, when PSf loading is increased to 6%, and 8% the broadening of signature peaks of cellulose triacetate was observed which refers to the decrement of crystallinity of blend membrane[40].

### 5.3 Ultimate Tensile Strength (UTS) Analysis

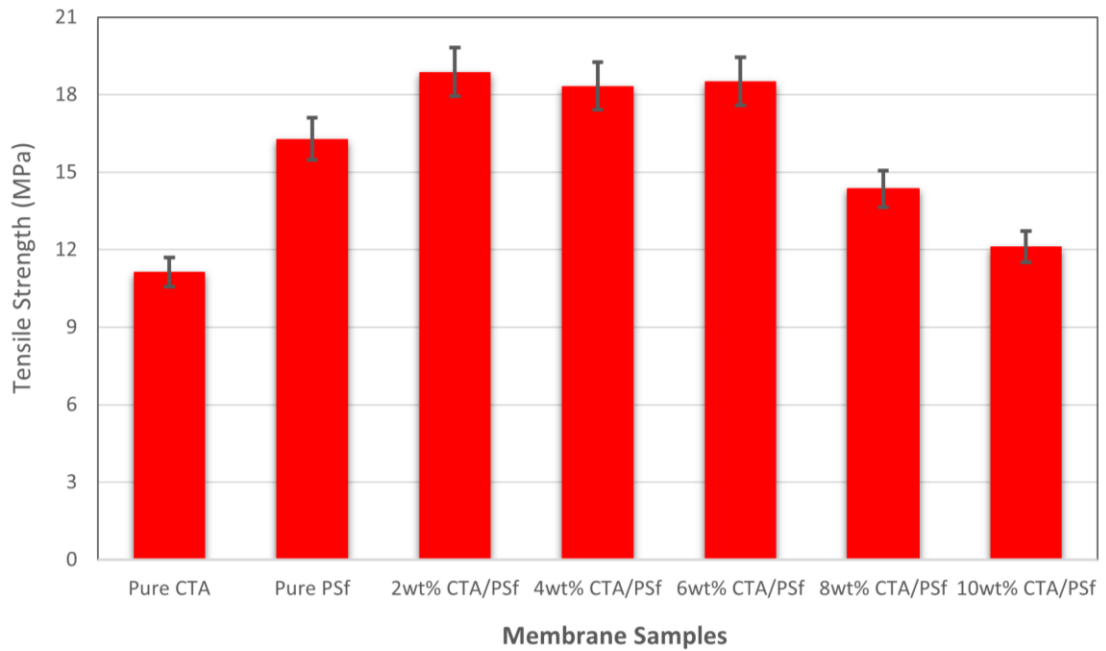


**Figure 5.3:** Ultimate Tensile Strength Results of Pristine CTA, PSf, and CTA/PSf Blend Membranes

Mechanical strength of the fabricated membrane was evaluated using UTM. In this characterization technique sample of 10mm\*26mm of membrane area was taken. Ultimate tensile strength is measured at 0.5 mm/min optimal elongation rate[50].

Tensile strengths of pristine membrane samples of CTA and PSf were around 11.13MPa and 16.22MPa, respectively, because in this case study both the polymers were crystalline in nature so that we can see that relatively more crystalline nature of PSf imparts higher strength in blended membrane as well, and when we increase the loading of PSf polymer to a certain limit of 8wt% matrix structure is disturbed and the tensile strength of matrix starts decreasing because blend is moving towards immiscibility, Tensile strengths of the blended membranes were represented in the table 5.1.

**Table 5.1:** UTS Results for different membrane samples

<b>Samples</b>	<b>Strength (MPa)</b>
Sample 1(CTA)	11.13395
Sample 2(PSf)	16.221
2wt% CTA/PSf	18.8753
4wt% CTA/PSf	18.3357
6wt% CTA/PSf	18.5149
8wt% CTA/PSf	14.3488
10wt% CTA/PSf	12.12141

In the comparison table 5.2 of blended membranes, we can see that by adding a small quantity of polysulfone polymer, the tensile strengths of the membrane samples were increased to a higher value. Nevertheless, the tensile strength decreases to a lower value of 12.12 MPa at 10% blended membrane as compared to pristine Cellulose triacetate membrane with 0% PSf[51].

According to the research, [52]the disruption or stiffness at the polymer interface occurs if we increase the filler loading to a certain amount. As the region around the filler polymer is stiffer as compared to the main membrane matrix, it will result in a decrease in the mechanical strength of the membrane.

#### **5.4 Scanning Electron Microscopy (SEM) Analysis**

Surface micrographs of all the membrane samples which contain the main matrix of Cellulose triacetate CTA with varying concentrations of Polysulfone PSf as polymeric filler i.e., 2,4,6,8, and 10wt% are represented in Figures 5.4. SEM images of all the membranes were taken at 1,000x magnification ranges. Initially, pristine cellulose triacetate and polysulfone membranes depict the dense and closely packed, symmetrical membrane structure as shown. Moving towards surface micrographs of

blended membranes of 2wt %, 4wt % and 6wt % PSf filler, we can easily see the smooth surface signifying a dense and defect free CTA matrix along with evenly distributed smaller dots like formations of PSf filler, which are visible in all the samples, as we go progressively from 2wt% to 6wt% in 8wt% and 10wt% we can see that the bubble like formation grow in size as well as in numbers, which confirms that larger loadings of polysulfone has been properly and successfully incorporated into the Cellulose triacetate matrix[39], [53].

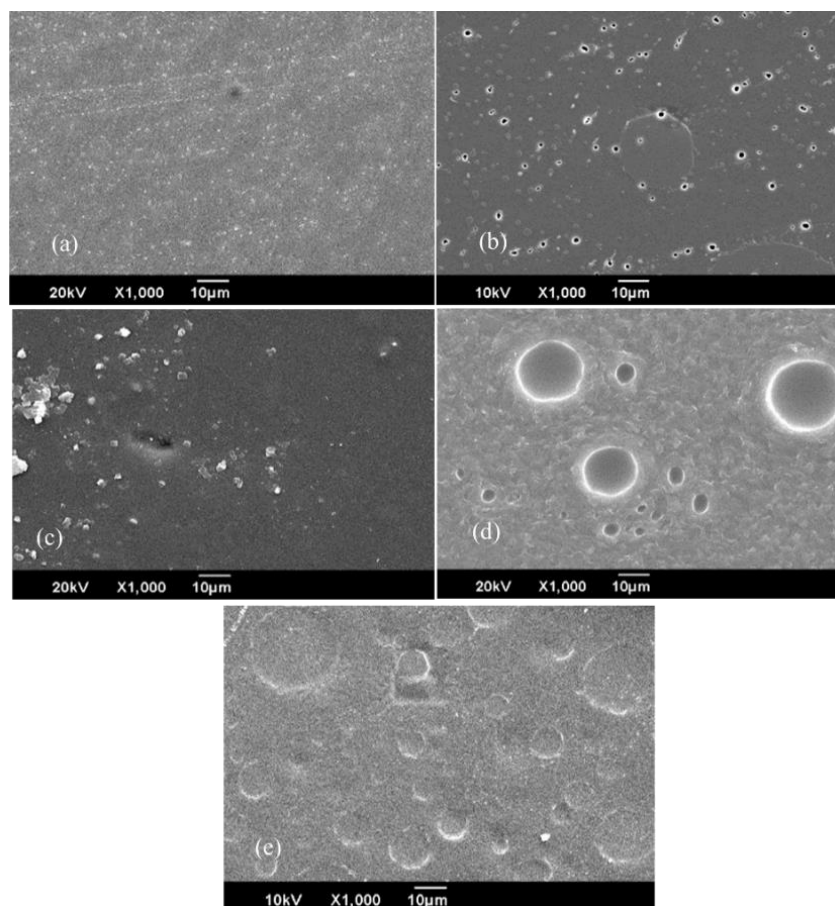


**Figure 5.4:** SEM surface micrographs of (A)= 2wt% CTA/PSf, (B)= 4wt% CTA/PSf, (C)= 6wt% CTA/PSf, (D)= 8wt% CTA/PSf, (E)= 10wt% CTA/PSf

Moreover, it also shows that a limit reaches, for the solubility of CTA and PSf with one another, and this limit is reached once the loading of PSf reached up to 10wt%.

Cross-sectional Morphology of all the fabricated membranes is shown in Figure 5.5. We can see clearly that all the fabricated membranes were dense, and defect free, no pores or cracks are shown in the cross-sectional micrographs which confirms



the dense and defect free structure of PSf/CTA blend membranes, although agglomeration is started at 8wt% and 10wt% PSf/CTA blends but it does not disturb the structure of membrane matrix[38]. Because of the extraction of nodules, which is the result of high interfacial tension and coalescence, the SEM images also showed that there were cavities present in the cross-section of the CTA/PSf 10wt% membrane. These holes were found because of the membrane's composition[40].

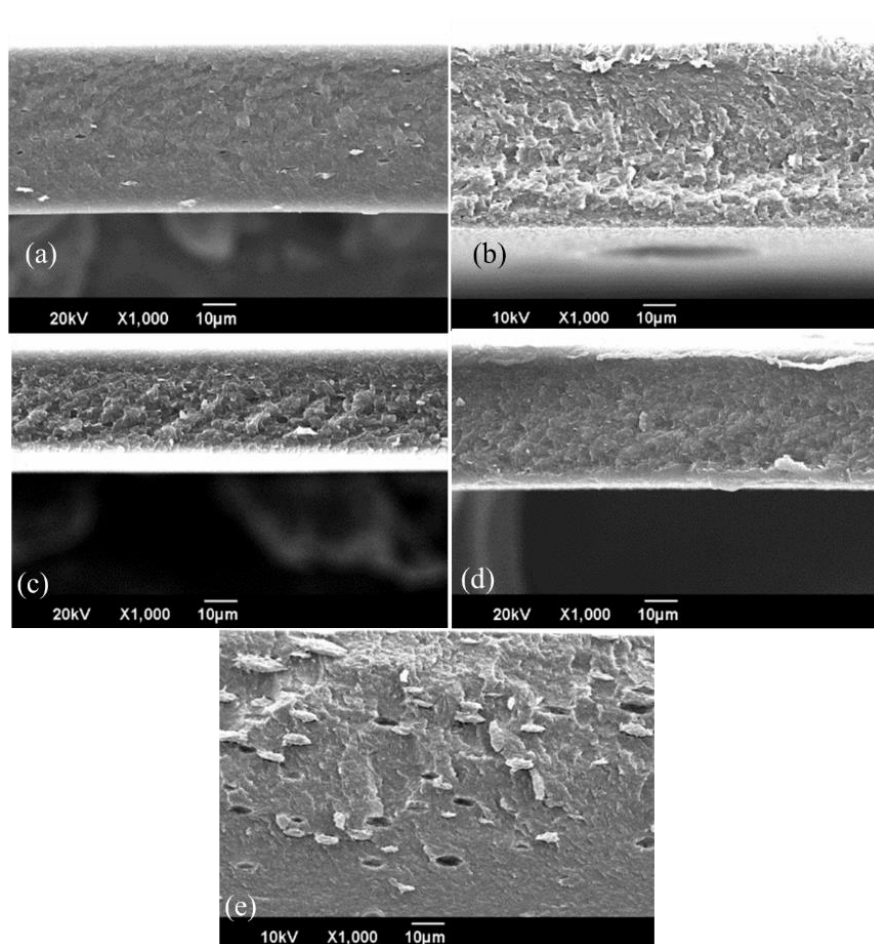


**Figure 5.5:** SEM Cross-Sectional micrographs of (A)= 2wt% CTA/PSf, (B)= 4wt% CTA/PSf, (C)= 6wt% CTA/PSf, (D)= 8wt% CTA/PSf, (E)= 10wt% CTA/PSf

## 5.5 Gas Permeation Analysis

All the pristine and blended membrane samples of CTA (100%), PSf (100%), 2%,4%, 6%, and 8% PSf in 1gm of CTA were assessed for single gas permeation test, using a stainless-steel gas permeation equipment (rig), at succeeding pressures of 2,3,4, and 5 bars, respectively. Single gas permeation results of CO<sub>2</sub> and CH<sub>4</sub> are summarized in the table 5.2:

**Table 5.2:** Gas Permeation Results

Membrane sample	Pressure (bars)	Permeability of CO <sub>2</sub> (Barrer)	Permeability of CH <sub>4</sub> (Barrer)	Selectivity CO <sub>2</sub> /CH <sub>4</sub>
CTA Pure	2	25.91	3.36	7.70
	3	16.68	1.95	8.54
	4	13.49	1.37	9.82
	5	10.97	1.66	6.57
PSf Pure	2	16.83	2.00	8.37
	3	12.11	1.09	11.04
	4	9.62	0.93	10.35
	5	11.17	0.90	12.41
2wt% CTA/PSf	2	14.58	1.85	7.84
	3	8.09	0.95	8.43
	4	7.70	0.76	10.04
	5	8.91	0.62	14.36
4wt% CTA/PSf	2	15.99	1.32	12.08
	3	14.35	0.75	18.90
	4	13.25	0.55	24.00
	5	15.52	0.60	25.70
6wt% CTA/PSf	2	12.79	1.06	11.98
	3	10.48	0.54	19.37
	4	<b>11.12</b>	<b>0.36</b>	<b>30.70</b>
	5	9.41	0.31	29.75
8wt% CTA/PSf	2	9.09	2.68	3.38
	3	11.35	1.43	7.89
	4	8.50	1.09	7.76
	5	7.13	1.02	6.98

Gas permeation results shown in the graph show that the permeability of gases decreases with the increase in pressure from 2,3,4, to 5 bar, respectively[54]. This decrease in permeability of gases can be explained by the phenomena of compression of membrane matrix on increased pressure.

Also, on higher loading of polymer B (PSf), which is more crystalline in nature as compared to CTA will make the main matrix stiffer and the polymer chains become more rigid, and less mobile because of that more steric hindrance is faced by the gas molecules, and permeability is diminished. So, selectivity of PSf/CTA blend of 2wt%-8wt% is increased because of some interactions between S=O group of PSf and CTA matrix[55].

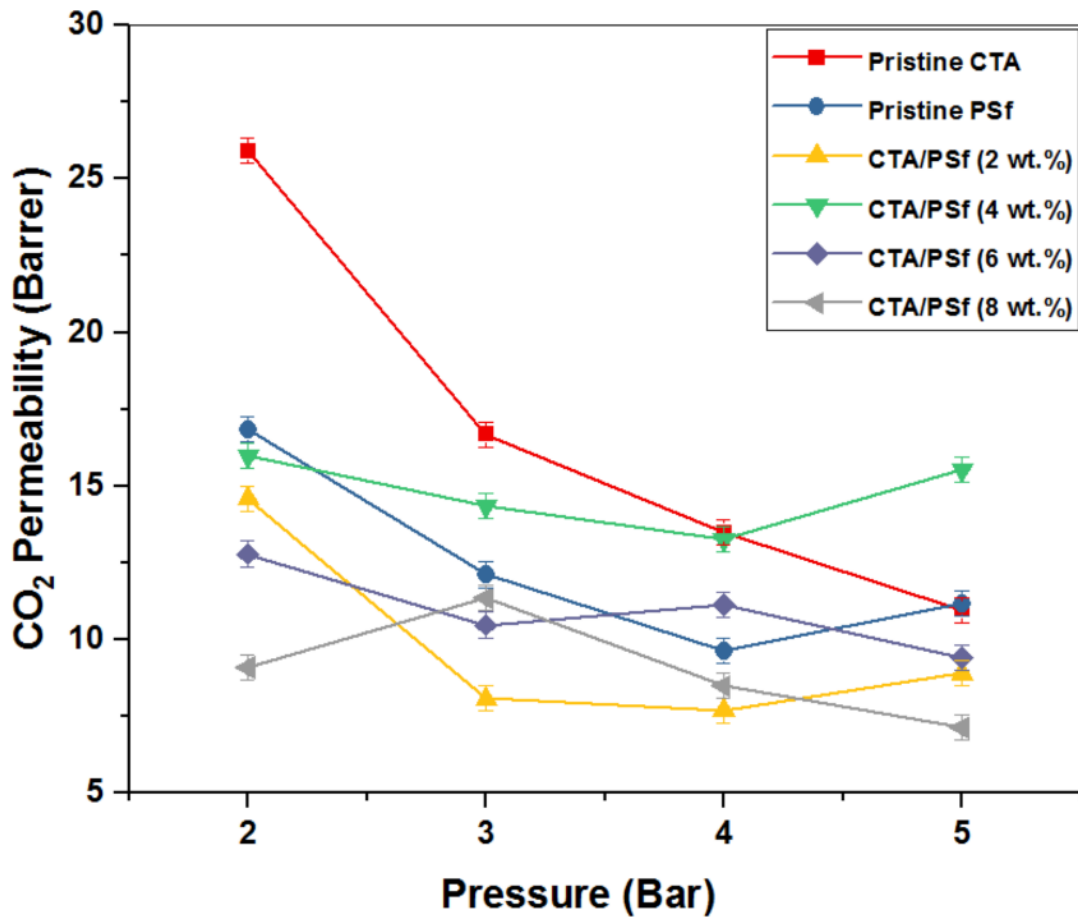
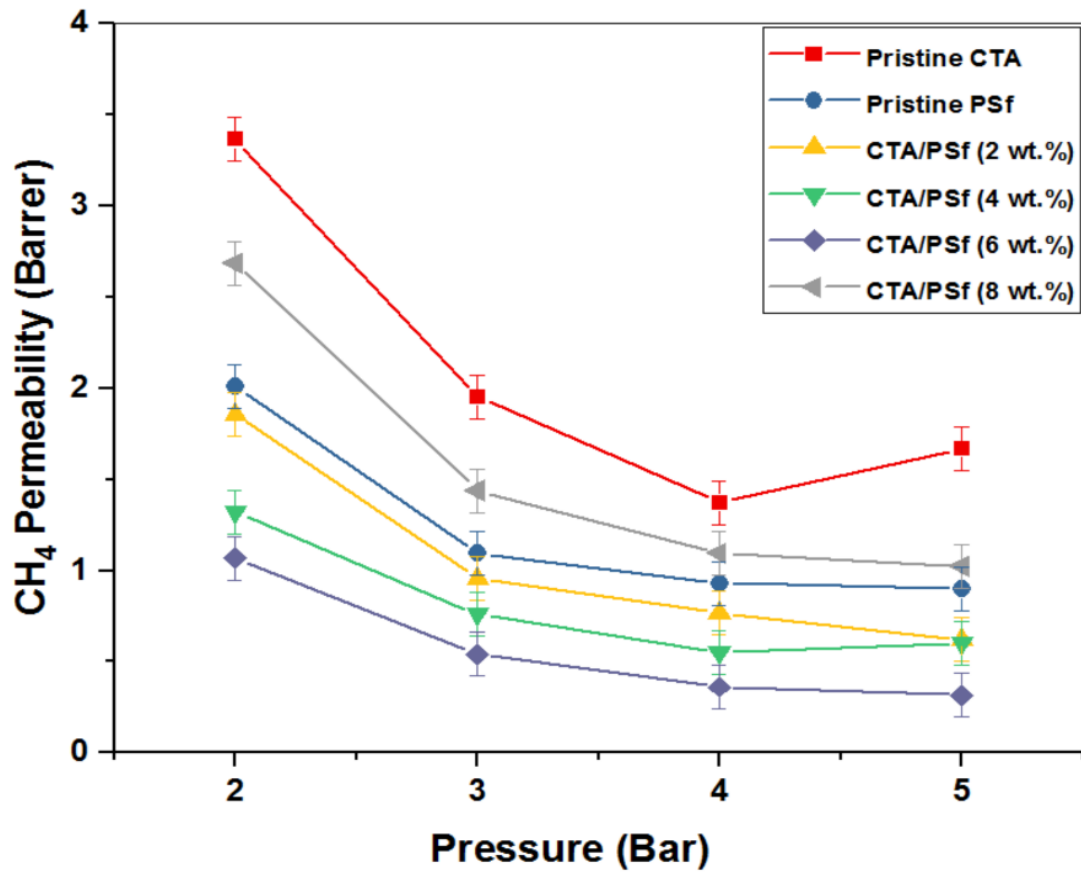


Figure 5.6: Permeabilities of CO<sub>2</sub>



**Figure 5.7:** Permeabilities of CH<sub>4</sub>

Idea selectivity (CO<sub>2</sub>/CH<sub>4</sub>) results of different blended membrane are represented in the fig below:

Based on ideal selectivity for various polymer blends it was found that the highest CO<sub>2</sub>/CH<sub>4</sub> selectivity of 30.70 and 25.70 was observed for 6wt% and 4wt% blend membranes as compared to the pristine membrane samples of CTA and PSf, which was around 7.7 to 9.8 and 8.37 to 12.41, respectively[40], [56].

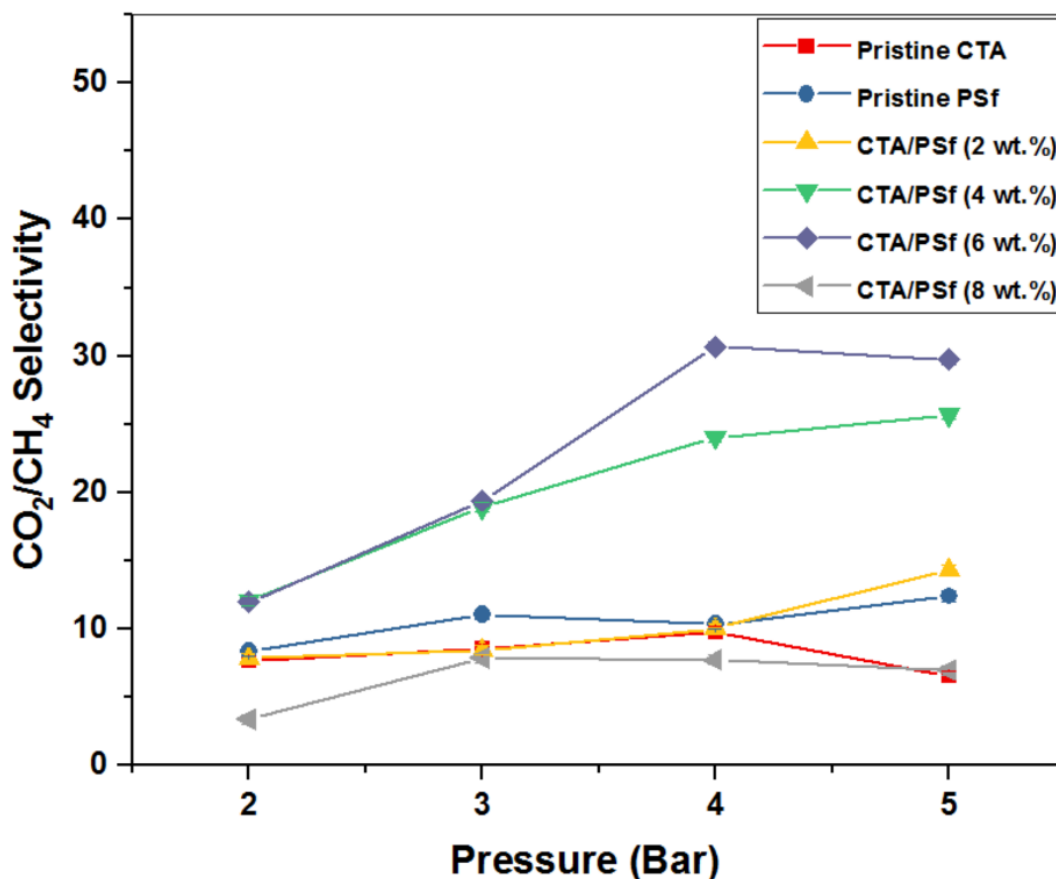


**Figure 5.8:** Selectivity of CO<sub>2</sub>/CH<sub>4</sub>

Overall, based on permeation, selectivity, and other characterization techniques it can be said that the polymer blend of CTA/PSf 6wt% was the best optimized sample.

## 5.6 Performance Comparison

A Robeson's upper bound curve is considered as a benchmark for the assessment of the trade-off between ideal selectivity, and permeabilities of the membrane materials. All the membrane samples' performances were plotted on the Robeson's upper bound curve (2008), as represented in Figure 5.9. The fabricated samples of membranes exhibited promising results, with permeability values that approached those predicted by the Robeson's upper bound curve. Also, the selectivity of the samples was also impressive, demonstrating a favorable balance between permeability and the ability to selectively separate specific gases[38], [40].

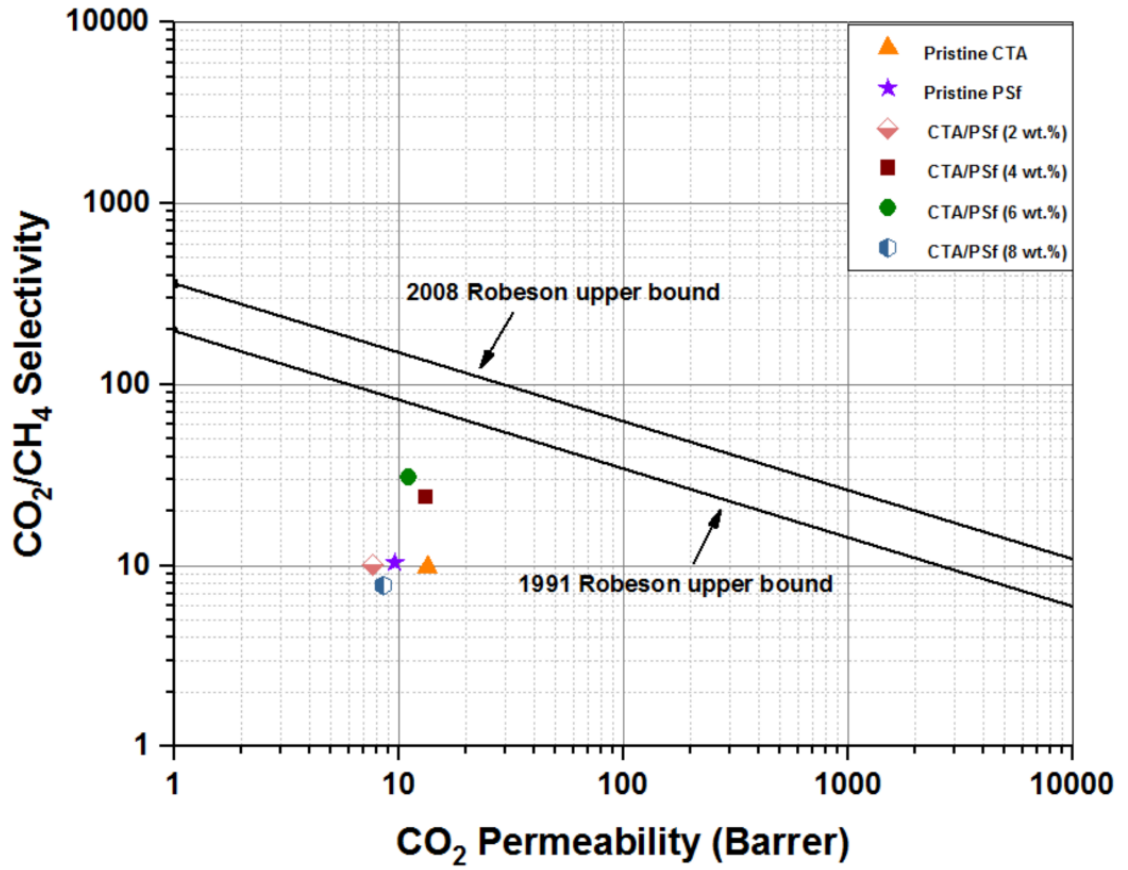


**Figure 5.9:** Performance comparison graph for all the samples prepared.

## CHAPTER 6: CONCLUSION

In conclusion, the present research focused on the fabrication and characterization of flat sheet membranes by blending polysulfone and cellulose triacetates with 2.84 degrees of acetylation.

The gas permeation study focused on CO<sub>2</sub> and CH<sub>4</sub> separation using a single gas testing apparatus from 2 bar to 5 bars feed pressure. The blending of CTA and PSf resulted in a noteworthy enhancement in CO<sub>2</sub>/CH<sub>4</sub> selectivity, escorted by a slight reduction in permeability compared to pristine Cellulose triacetate membranes. In spite of reduction in permeability, the combination of selectivity and permeability values for blend membranes caused the blend membranes to move closer to the Robeson upper bound as compared to pristine polymers. The separation performance of all the fabricated membrane samples was assessed based on Robeson's upper bound curve (2008). Among the membranes evaluated, the CTA/PSf (6wt%) blended sample exhibited notable performance, positioning it favorably on Robeson's upper bound curve. It demonstrated a CO<sub>2</sub> permeability of 11.12 Barrer and a CO<sub>2</sub>/CH<sub>4</sub> selectivity of 30.70.

Compared to the pristine CTA membrane, the optimal blended membrane highlighted a remarkable 98% enhancement in CO<sub>2</sub>/CH<sub>4</sub> selectivity while experiencing only a 6% reduction in CO<sub>2</sub> permeability. These results highlight the potential of the fabricated membranes for effective CO<sub>2</sub> and CH<sub>4</sub> separation. The findings contribute to the advancement of membrane technology for various industrial applications, including natural gas purification, and carbon capture. The developed membranes hold promises for addressing environmental concerns and facilitating sustainable energy processes. Further research and optimization of the blended membranes are warranted to realize their full potential in practical gas separation applications.

The characterization results obtained through FTIR, XRD, UTM, and SEM techniques confirmed the formation of homogeneous blends with better interfacial interaction, resulting in dense and defect-free membranes. SEM analysis revealed an asymmetric structure for all CTA/PSf blended membranes, with loosely packed regions between dense skin layers. FTIR analysis provided evidence of physical

interaction between the cellulose triacetate and polysulfone polymers, indicating their compatibility and blend formation. UTM results demonstrated significant improvements in the tensile strength and stiffness of the membranes due to the blending process.



## REFERENCES

- [1] “S&P Global Commodity Insights.” <https://www.spglobal.com/commodityinsights/en/market-insights/latest-news/oil/100621-global-energy-demand-to-grow-47-by-2050-with-oil-still-top-source-us-eia#:~:text=14%3A20%20UTC-,Global%20energy%20demand%20to%20grow%2047%25%20by%202050%2C%20with%20oil,still%20top%20source%3A%20US%20EIA&text=Global%20energy%20demand%20and%20energy,Energy%20Information%20Administration%20said%20Oct.> (accessed Aug. 31, 2023).
- [2] I. Energy Agency, “Electricity Market Report – December 2020,” 2020.
- [3] “Pakistan Energy Information.” <https://www.enerdata.net/estore/energy-market/pakistan/#:~:text=Crude%20Oil%20Production,Mt%20in%202019%20and%202020.> (accessed Aug. 31, 2023).
- [4] M. Hassanpour, “O<sub>2</sub>, N<sub>2</sub>, CO, CO<sub>2</sub> Capture Technologies in the Post-Combustion Operation of the Waste Stream (A Review),” Article in International Journal of Waste Resources, 2021, doi: 10.35248/2252-5211.21.11.396.
- [5] M. M. Zagho, M. K. Hassan, M. Khraisheh, M. A. A. Al-Maadeed, and S. Nazarenko, “A review on recent advances in CO<sub>2</sub> separation using zeolite and zeolite-like materials as adsorbents and fillers in mixed matrix membranes (MMMs),” Chemical Engineering Journal Advances, vol. 6, May 2021, doi: 10.1016/j.ceja.2021.100091.
- [6] D. D. Iarikov and S. Ted Oyama, Review of CO<sub>2</sub>/CH<sub>4</sub> Separation Membranes, vol. 14. 2011. doi: 10.1016/B978-0-444-53728-7.00005-7.
- [7] D. D. Iarikov and S. Ted Oyama, Review of CO<sub>2</sub>/CH<sub>4</sub> Separation Membranes, vol. 14. 2011. doi: 10.1016/B978-0-444-53728-7.00005-7.
- [8] Y. W. Jeon and D. H. Lee, “Gas membranes for CO<sub>2</sub>/CH<sub>4</sub> (biogas) separation: A review,” Environmental Engineering Science, vol. 32, no. 2. Mary Ann Liebert Inc., pp. 71–85, Feb. 01, 2015. doi: 10.1089/ees.2014.0413.

- [9] “gsmblog.” <https://gsmblog-us.fujifilm.com/blog/gas-separation-membrane-history/> (accessed Aug. 31, 2023).
- [10] H. Lin and M. Yavari, “Upper bound of polymeric membranes for mixed-gas CO<sub>2</sub>/CH<sub>4</sub> separations,” *J Memb Sci*, vol. 475, pp. 101–109, Feb. 2015, doi: 10.1016/j.memsci.2014.10.007.
- [11] M. Chawla et al., “Membranes for CO<sub>2</sub> /CH<sub>4</sub> and CO<sub>2</sub>/N<sub>2</sub> Gas Separation,” *Chemical Engineering and Technology*, vol. 43, no. 2. Wiley-VCH Verlag, pp. 184–199, Feb. 01, 2020. doi: 10.1002/ceat.201900375.
- [12] M. Sinaei Nobandegani, L. Yu, and J. Hedlund, “Zeolite membrane process for industrial CO<sub>2</sub>/CH<sub>4</sub> separation,” *Chemical Engineering Journal*, vol. 446, Oct. 2022, doi: 10.1016/j.cej.2022.137223.
- [13] Z. Salahuddin, S. Farrukh, A. Hussain, T. Noor, and W. Kwapinski, “Mixed and single gas permeation performance analysis of amino-modified ZIF based mixed matrix membrane,” *Polymers and Polymer Composites*, vol. 29, no. 9\_suppl, pp. S707–S718, Nov. 2021, doi: 10.1177/09673911211023303.
- [14] N. Jusoh, Y. F. Yeong, T. L. Chew, K. K. Lau, and A. M. Shariff, “Current Development and Challenges of Mixed Matrix Membranes for CO<sub>2</sub>/CH<sub>4</sub> Separation,” *Separation and Purification Reviews*, vol. 45, no. 4. Taylor and Francis Inc., pp. 321–344, Oct. 01, 2016. doi: 10.1080/15422119.2016.1146149.
- [15] T. D. Kusworo, A. F. Ismail, and A. Mustafa, “EXPERIMENTAL DESIGN AND RESPONSE SURFACE MODELING OF PI/PES-ZEOLITE 4A MIXED MATRIX MEMBRANE FOR CO<sub>2</sub> SEPARATION,” 2015.
- [16] Y. Zhang, K. J. Balkus, I. H. Musselman, and J. P. Ferraris, “Mixed-matrix membranes composed of Matrimid® and mesoporous ZSM-5 nanoparticles,” *J Memb Sci*, vol. 325, no. 1, pp. 28–39, Nov. 2008, doi: 10.1016/j.memsci.2008.04.063.
- [17] A. Ebadi Amooghin, M. Omidkhan, and A. Kargari, “Enhanced CO<sub>2</sub> transport properties of membranes by embedding nano-porous zeolite particles into Matrimid®5218 matrix,” *RSC Adv*, vol. 5, no. 12, pp. 8552–8565, 2015, doi: 10.1039/c4ra14903c.

- [18] M. Rezakazemi, I. Heydari, and Z. Zhang, “Hybrid systems: Combining membrane and absorption technologies leads to more efficient acid gases (CO<sub>2</sub> and H<sub>2</sub>S) removal from natural gas,” *Journal of CO<sub>2</sub> Utilization*, vol. 18, pp. 362–369, Mar. 2017, doi: 10.1016/j.jcou.2017.02.006.
- [19] M. M. Birgül Tantekin-Ersolmaz, L. L. Lara, senorkyan, N. Kalaonra, M. Tatlier, A. Ay, se, and E.-, Senatalar, “n-Pentane/i-pentane separation by using zeolite-PDMS mixed matrix membranes,S,” 2001.
- [20] F. Moghadam, M. R. Omidkhah, E. Vasheghani-Farahani, M. Z. Pedram, and F. Dorosti, “The effect of TiO<sub>2</sub> nanoparticles on gas transport properties of Matrimid5218-based mixed matrix membranes,” *Sep Purif Technol*, vol. 77, no. 1, pp. 128–136, Feb. 2011, doi: 10.1016/j.seppur.2010.11.032.
- [21] C. Y. Liang et al., “A comparison on gas separation between PES (polyethersulfone)/MMT (Na-montmorillonite) and PES/TiO<sub>2</sub> mixed matrix membranes,” in *Separation and Purification Technology*, May 2012, pp. 57–63. doi: 10.1016/j.seppur.2012.03.016.
- [22] Q. Hu, E. Marand ’, S. Dhingra, D. Fritsch, J. Wen, and G. Wilkes, “Poly(amide-imide)/TiO<sub>2</sub> nano-composite gas separation membranes" Fabrication and characterization,” 1997.
- [23] B. Lam et al., “Cellulose triacetate doped with ionic liquids for membrane gas separation,” *Polymer (Guildf)*, vol. 89, pp. 1–11, Apr. 2016, doi: 10.1016/j.polymer.2016.02.033.
- [24] H. R. Mahdavi, N. Azizi, M. Arzani, and T. Mohammadi, “Improved CO<sub>2</sub>/CH<sub>4</sub> separation using a nanocomposite ionic liquid gel membrane,” *J Nat Gas Sci Eng*, vol. 46, pp. 275–288, Oct. 2017, doi: 10.1016/j.jngse.2017.07.024.
- [25] M. Bhattacharya and M. K. Mandal, “Synthesis and characterization of ionic liquid based mixed matrix membrane for acid gas separation,” *J Clean Prod*, vol. 156, pp. 174–183, Jul. 2017, doi: 10.1016/j.jclepro.2017.04.034.
- [26] P. Tanvidkar, A. Jonnalagedda, and B. V. R. Kuncharam, “Investigation of cellulose acetate and ZIF-8 mixed matrix membrane for CO<sub>2</sub> separation from model biogas,” *Environmental Technology (United Kingdom)*, 2023, doi: 10.1080/09593330.2023.2192366.

- [27] J. Li, S. Wang, K. Nagai, T. Nakagawa, and A. W. H. Mau, "Effect of polyethyleneglycol (PEG) on gas permeabilities and permselectivities in its cellulose acetate (CA) blend membranes," *J Memb Sci*, vol. 138, no. 2, pp. 143–152, Jan. 1998, doi: 10.1016/S0376-7388(97)00212-3.
- [28] A. R. Moghadassi, Z. Rajabi, S. M. Hosseini, and M. Mohammadi, "Fabrication and modification of cellulose acetate based mixed matrix membrane: Gas separation and physical properties," *Journal of Industrial and Engineering Chemistry*, vol. 20, no. 3, pp. 1050–1060, May 2014, doi: 10.1016/j.jiec.2013.06.042.
- [29] C. Yi, Z. Wang, M. Li, J. Wang, and S. Wang, "Facilitated transport of CO<sub>2</sub> through polyvinylamine/polyethylene glycol blend membranes," *Desalination*, vol. 193, no. 1–3, pp. 90–96, May 2006, doi: 10.1016/j.desal.2005.04.139.
- [30] A. Y. Houde, B. Krishnakumar, S. G. Charati, S. A. Stern, and J. Wiley, "Permeability of Dense (Homogeneous) Cellulose Acetate Membranes to Methane, Carbon Dioxide, and Their Mixtures at Elevated Pressures."
- [31] Y. Cai, Z. Wang, C. Yi, Y. Bai, J. Wang, and S. Wang, "Gas transport property of polyallylamine–poly(vinyl alcohol)/polysulfone composite membranes," *J Memb Sci*, vol. 310, no. 1–2, pp. 184–196, Mar. 2008, doi: 10.1016/J.MEMSCI.2007.10.052.
- [32] A. F. Ismail and W. Lorna, "Penetrant-induced plasticization phenomenon in glassy polymers for gas separation membrane," *Sep Purif Technol*, vol. 27, no. 3, pp. 173–194, Jun. 2002, doi: 10.1016/S1383-5866(01)00211-8.
- [33] D. Wang, W. K. Teo, and K. Li, "Preparation and characterization of high-flux polysulfone hollow fibre gas separation membranes," 2002.
- [34] S. Kim, S. H. Han, and Y. M. Lee, "Thermally rearranged (TR) polybenzoxazole hollow fiber membranes for CO<sub>2</sub> capture," *J Memb Sci*, vol. 403–404, pp. 169–178, Jun. 2012, doi: 10.1016/J.MEMSCI.2012.02.041.
- [35] C. Cao, T. S. Chung, Y. Liu, R. Wang, and K. P. Pramoda, "Chemical cross-linking modification of 6FDA-2,6-DAT hollow fiber membranes for natural gas separation," *J Memb Sci*, vol. 216, no. 1–2, pp. 257–268, May 2003, doi: 10.1016/S0376-7388(03)00080-2.

- [36] “Chemical-structures-of-cellulose-and-cellulose-triacetate-CTA”.
- [37] “Chemical-structure-of-polysulfone-PSf-diaminodiphenyl-sulfone-DDS-and”.
- [38] A. Raza, S. Japip, C. Z. Liang, S. Farrukh, A. Hussain, and T. S. Chung, “Novel cellulose triacetate (Cta)/cellulose diacetate (cda) blend membranes enhanced by amine functionalized zif-8 for CO<sub>2</sub> separation,” *Polymers (Basel)*, vol. 13, no. 17, Sep. 2021, doi: 10.3390/polym13172946.
- [39] I. Douna et al., “Experimental investigation of polysulfone modified cellulose acetate membrane for CO<sub>2</sub>/H<sub>2</sub> gas separation,” *Korean Journal of Chemical Engineering*, vol. 39, no. 1, pp. 189–197, Jan. 2022, doi: 10.1007/s11814-021-0900-7.
- [40] A. Raza, S. Farrukh, A. Hussain, I. Khan, M. H. D. Othman, and M. Ahsan, “Performance analysis of blended membranes of cellulose acetate with variable degree of acetylation for CO<sub>2</sub>/CH<sub>4</sub> separation,” *Membranes (Basel)*, vol. 11, no. 4, Apr. 2021, doi: 10.3390/membranes11040245.
- [41] A. R. Moghadassi, Z. Rajabi, S. M. Hosseini, and M. Mohammadi, “Fabrication and modification of cellulose acetate based mixed matrix membrane: Gas separation and physical properties,” *Journal of Industrial and Engineering Chemistry*, vol. 20, no. 3, pp. 1050–1060, May 2014, doi: 10.1016/J.JIEC.2013.06.042.
- [42] P. D. Sutrisna, E. Savitri, M. A. Gunawan, I. H. F. Putri, and S. G. B. de Rozari, “Synthesis, characterization, and gas separation performances of polysulfone and cellulose acetate-based mixed matrix membranes,” *Polymer-Plastics Technology and Materials*, vol. 59, no. 12, pp. 1300–1307, Aug. 2020, doi: 10.1080/25740881.2020.1738471.
- [43] Y. Alqaheem and A. A. Alomair, “Microscopy and spectroscopy techniques for characterization of polymeric membranes,” *Membranes (Basel)*, vol. 10, no. 2, Feb. 2020, doi: 10.3390/MEMBRANES10020033.
- [44] B. Tylkowski and I. Tsibranska, “Overview of main techniques used for membrane characterization,” 2015.

- [45] M. Ionita, L. E. Crica, S. I. Voicu, A. M. Pandeale, and H. Iovu, "Fabrication of cellulose triacetate/graphene oxide porous membrane," *Polym Adv Technol*, vol. 27, no. 3, pp. 350–357, Mar. 2016, doi: 10.1002/pat.3646.
- [46] T. P. N. Nguyen, E. T. Yun, I. C. Kim, and Y. N. Kwon, "Preparation of cellulose triacetate/cellulose acetate (CTA/CA)-based membranes for forward osmosis," *J Memb Sci*, vol. 433, pp. 49–59, Apr. 2013, doi: 10.1016/j.memsci.2013.01.027.
- [47] Y. Liu, Z. Liu, A. Morisato, N. Bhuvania, D. Chinn, and W. J. Koros, "Natural gas sweetening using a cellulose triacetate hollow fiber membrane illustrating controlled plasticization benefits," *J Memb Sci*, vol. 601, Mar. 2020, doi: 10.1016/j.memsci.2020.117910.
- [48] D. Zavastin et al., "Preparation, characterization and applicability of cellulose acetate-polyurethane blend membrane in separation techniques," *Colloids Surf A Physicochem Eng Asp*, vol. 370, no. 1–3, pp. 120–128, Nov. 2010, doi: 10.1016/j.colsurfa.2010.08.058.
- [49] A. Y. Houde, B. Krishnakumar, S. G. Charati, S. A. Stern, and J. Wiley, "Permeability of Dense (Homogeneous) Cellulose Acetate Membranes to Methane, Carbon Dioxide, and Their Mixtures at Elevated Pressures."
- [50] G. C. Kapantaidakis, S. P. Kaldis, X. S. Dabou, and G. P. Sakellaropoulos, "Gas permeation through PSf-PI miscible blend membranes," 1996.
- [51] H. Abdul Mannan, H. Mukhtar, M. Shima Shaharun, M. Roslee Othman, and T. Murugesan, "Polysulfone/poly(ether sulfone) blended membranes for CO<sub>2</sub> separation," *J Appl Polym Sci*, vol. 133, no. 5, Feb. 2016, doi: 10.1002/app.42946.
- [52] H. Julian, "Polysulfone membranes for CO<sub>2</sub>/CH<sub>4</sub> separation: State of the art," *IOSR Journal of Engineering*, vol. 02, no. 03, pp. 484–495, Mar. 2012, doi: 10.9790/3021-0203484495.
- [53] I. Douna, S. Farrukh, E. Pervaiz, A. Hussain, X. F. Fan, and Z. Salahuddin, "Blending of ZnO Nanorods in Cellulose Acetate Mixed Matrix Membrane for Enhancement of CO<sub>2</sub> Permeability," *J Polym Environ*, vol. 31, no. 6, pp. 2549–2565, Jun. 2023, doi: 10.1007/s10924-022-02594-z.

- [54] M. A. Aroon, A. F. Ismail, M. M. Montazer-Rahmati, and T. Matsuura, "Morphology and permeation properties of polysulfone membranes for gas separation: Effects of non-solvent additives and co-solvent," *Sep Purif Technol*, vol. 72, no. 2, pp. 194–202, Apr. 2010, doi: 10.1016/j.seppur.2010.02.009.
- [55] N. Azizi, M. R. Hojjati, and M. M. Zarei, "Study of CO<sub>2</sub> and CH<sub>4</sub> Permeation Properties through Prepared and Characterized Blended Pebax-2533/PEG-200 Membranes," *Silicon*, vol. 10, no. 4, pp. 1461–1467, Jul. 2018, doi: 10.1007/s12633-017-9626-x.
- [56] C. Regmi, S. Ashtiani, Z. Sofer, and K. Friess, "Improved CO<sub>2</sub>/CH<sub>4</sub> separation properties of cellulose triacetate mixed–matrix membranes with ceo2@go hybrid fillers," *Membranes (Basel)*, vol. 11, no. 10, Oct. 2021, doi: 10.3390/membranes11100777.